

The physics of active polymers and filaments

Roland G. Winkler and Gerhard Gompper^{a)}

(Dated: 25 June 2020)

Active matter agents consume internal energy or extract energy from the environment for locomotion and force generation. Already rather generic models, such as ensembles of active Brownian particles, exhibit phenomena, which are absent at equilibrium, in particular motility-induced phase separation and collective motion. Further intriguing nonequilibrium effects emerge in assemblies of bound active agents as in linear polymers or filaments. The interplay of activity and conformational degrees of freedom gives rise to novel structural and dynamical features of individual polymers as well as in interacting ensembles. Such out-of-equilibrium polymers are an integral part of living matter, ranging from biological cells with filaments propelled by motor proteins in the cytoskeleton, and RNA/DNA in the transcription process, to long swarming bacteria and worms such as *Proteus mirabilis* and *Caenorhabditis elegans*, respectively. Even artificial active polymers have been synthesized. The emergent properties of active polymers or filaments depend on the coupling of the active process to their conformational degrees of freedom, aspects which are addressed in this article. The theoretical models for tangentially and isotropically self-propelled or active-bath driven polymers are presented, both in presence and absence of hydrodynamic interactions. The consequences for their conformational and dynamical properties are examined, emphasizing the strong influence of the coupling between activity and hydrodynamic interactions. Particular features of emerging phenomena, induced by steric and hydrodynamic interactions, are highlighted. Various important, yet theoretically unexplored, aspects are featured and future challenges are discussed.

I. INTRODUCTION

Living matter is characterized by a multitude of complex dynamical processes maintaining its out-of-equilibrium nature.^{1,2} Molecular machines such as (motor) proteins and ribosomes undergo conformational changes fueled by Adenosine Triphosphate (ATP), which drive and stir the cell interior.^{3,4} This triggers a hierarchy of dynamical processes, movements, and transport, resulting in a nonequilibrium state of the cell—from the molecular to the whole-cell level—,² with intriguing collective phenomena emerging by migration and locomotion also on scales much larger than individual cells.^{5–9} The nature of living and active matter systems implies nonthermal fluctuations, broken detailed balance, and a violation of the dissipation-fluctuation relation, which renders their theoretical description particularly challenging.²

Filaments and polymers are an integral part of biological systems, and their conformational and dynamical properties are substantially affected by the active processes to a yet unresolved extent.

Biological active polymers and filaments — Enzymatic conformational changes are considered to induce fluctuating hydrodynamic flows in the cytoplasm, which lead to an enhanced diffusion of dissolved colloidal and polymeric objects.^{4,10–21} In addition, kinesin motors walking along microtubule filaments generate forces that affect the dynamics of the cytoskeletal network, the transport proper-

ties of species in the cell, and the organization of the cell interior.^{11,22–24} Even more, molecular motors give rise to nonequilibrium conformational fluctuations of actin filaments and microtubules.^{12,25}

Within the nucleus, ATPases such as DNA or RNA polymerase (RNAP, DNAP) are involved in DNA transcription, where the information coded in the base-pair sequence of DNA is transcribed into DNA or RNA. This proceeds in several steps, where the ATPases locally unzip the two DNA strands, nucleotides are added to the synthesized molecules, and the ATPases move along the DNA.²⁶ Hence, every RNAP/DNAP translocation step is a complex process, which generates nonthermal fluctuations for both, RNAP/DNAP as well as the transcribed DNA.^{26–28}

Various of these active process are considered to be involved in the spatial arrangement of the eukaryotic genome, controlling their dynamical properties, and being essential for the cell function.²⁹ In particular, ATP-dependent processes affect the dynamics of chromosomal loci^{19,30} and chromatin.³¹ Moreover, spatial segregation of active (euchromatin) and passive (heterochromatin) chromatin has been found.^{32–34} The detailed mechanism needs to be unraveled, possibly taking active processes into account.^{35,36}

Microswimmers are a particular class of active matter, where individual agents move autonomously by either converting internal chemical energy into directed motion, or utilizing energy from the environment.^{5,6,37–40} Biological microswimmers, like algae, sperm, and bacteria, are omnipresent.^{6,38,41} Numerous biological microswimmers are rather elongated and polymer- or filament-like, undergoing shape changes during migration. A particular example are elongated swarming bacteria, propelled by flagella, such as *Proteus mirabilis*, *Vibrio*

^{a)}Theoretical Physics of Living Matter, Institute of Biological Information Processing and Institute for Advanced Simulation, Forschungszentrum Jülich, D-52425 Jülich, Germany; Electronic mail: r.winkler@fz-juelich.de, g.gompper@fz-juelich.de

parahaemolyticus,^{42,43} or *Serratia marcescens*,⁴⁴ which exhibit an intriguing collective behavior. Other microswimmers organize in chain-like structures, for example planktonic dinoflagellates^{45,46} or *Bacillus subtilis* bacteria during biofilm formation.⁴⁷ On a more macroscopic scale, nematodes such as *Caenorhabditis elegans* swim⁴⁸ and collectively organize into dynamical networks.⁴⁹

Similarly, biological polar filaments like actin and microtubules driven by molecular motors exhibit filament bundling and the emergence of active turbulence, which is characterized by high vorticity and presence of motile topological defects.^{5,24,38,50–60}

These diverse aspects illustrate the relevance of activity for the function of cells and other biological polymer-like active objects. However, a cell is a very complex system with a multitude of concurrent processes, hence, a classification or the separation of individual active processes is difficult. Here, a systematic study of emergent phenomena due to activity by synthetic model systems may be useful. More importantly, the understanding of active processes and their suitable implementation may be essential in the rational design of synthetic cells.^{61–63}

Synthetic active polymers — Synthetic active or activated colloidal molecules⁶⁴ or polymers⁶⁵ are nowadays obtained in several ways.^{66,67} Various concepts have been put forward for the design of synthetic active particles, which can serve as monomers. Typically, propulsion is based on phoretic effects, relying on local gradients of, e.g., electric fields (electrophoresis), concentration (diffusiophoresis), and temperature (thermophoresis).^{39,68–76} Synthetic active systems exhibit a wide spectrum of novel and fascinating phenomena, specifically activity-driven phase separation or large-scale collective motion.^{5,6,37–39,77–80}

Catalytic Janus particles have been shown to spontaneously self-assemble into autonomously swimming dimers with a wide variety of morphologies.^{81,82} Assembly of metal-dielectric Janus colloids (monomers) into active chains can be achieved by imbalanced interactions, where the motility and the colloid interactions are simultaneously controlled by an AC electric field.^{83–88} Through the application of strong AC electric fields, linear chains of bound Janus particles can be achieved either by van-der-Waals forces or polymer linkers.⁸⁹ Electrohydrodynamic convection rolls lead to self-assembled colloidal chains in a nematic liquid crystal matrix and directed movement.⁹⁰ Linear self-assembly of dielectric colloidal particles is achieved by alternating magnetic fields, where the chain length can be controlled by the external field.^{91,92} Moreover, chains of linked colloids, which are uniformly coated with catalytic nanoparticles, have been synthesized.⁹³ Hydrogen peroxide decomposition on the surfaces of the colloidal monomers generates phoretic flows, and activity induced hydrodynamic interactions between monomers results in an enhanced diffusive motion.⁹³

Objectives — Filamentous and polymeric structures play a major role in biological systems and are heav-

ily involved in nonequilibrium processes. However, we are far from understanding the interplay between out-of-equilibrium fluctuations, corresponding polymer conformations, and emerging activity-driven self-organized structures. Studies of molecular/polymeric active matter will reveal original physical phenomena, and promote the development of novel smart devices and materials.

In this perspective article, we address the distinctive features emerging from the coupling of activity and conformational degrees of freedom of filamentous and polymeric structures. Assemblies of active colloidal particles have been denoted as *active colloidal molecules*.⁶⁴ Since we focus not only on synthetic colloidal systems, but also on polymers and filaments in biological systems, we will use the notion *active polymers*.⁶⁵

Different concepts for the active dynamics of polymers can be imagined or realized. For polymers composed of linearly connected monomers, the latter can be assumed to be themselves active, i.e., self-propelling, or to be activated, i.e., externally driven by a nonthermal force. Self-propulsion typically emerges by the interaction of a microswimmer with the embedding fluid. Here, hydrodynamics plays a major role and momentum is conserved. This is denoted as wet active matter. In contrast, dry active matter is characterized by the absence of local momentum conservation and, hence, hydrodynamic interactions. Here, other effects, such as strong particle-particle interactions or contact with a momentum-absorbing medium, as in bacteria gliding or granular beads vibrating on frictional surfaces, dominate over fluid-mediated interactions.⁹⁴ Moreover, externally-driven polymers are subject to forces, which, when they are dissolved in a fluid, give rise to Stokeslet flows and hydrodynamic interactions. Depending on the nature of the polymer environment, the emerging properties by the coupling of activity and the internal degrees of freedom can be rather different.^{88,95,96} Moreover, the nature of the active force determines the driving of a monomer. The forces on filaments driven by molecular motors are typically assumed to push them along the local filament tangent.^{6,60,97} Another realization are spatially independent, but time-correlated, active forces on monomers. We will highlight the impact of the various aspects—self-propelled vs. actuated, dry vs. wet, tangentially vs. randomly driven—on the polymer conformations, dynamics, and collective effects.

The article is organized as follows. Section II describes realizations of dry and wet active forces on the level of monomers and bonds. The properties of dry polymers composed of active Brownian particles are discussed in Sec. III. Effects of hydrodynamic interactions are included in Sec. IV. Section V is devoted to properties of tangentially driven dry polymers, and Sec. VI presents aspects of hydrodynamically self-propelled polymers. Collective effects are discussed in Sec. VII. Finally, Sec. VIII summarizes the major aspects and indicates possible future research directions.

II. ACTIVE FORCES

In models of active polymers, forces can directly be assigned to individual monomers, or to the bond connecting two monomers. This defines the minimal active units—either a monomer or a dumbbell of two connected monomers.

A. Active Brownian particles

A generic model of a self-propelled particle, especially suitable for dry active matter, is the well-known active Brownian particle (ABP).^{6,39,68,78,79,98–103} Its overdamped equations of motion are given by

$$\dot{\mathbf{r}}(t) = \frac{1}{\gamma_T} \mathbf{F}^a + \frac{1}{\gamma_T} (\mathbf{F}(t) + \boldsymbol{\Gamma}(t)), \quad (1)$$

$$\dot{\mathbf{e}}(t) = \boldsymbol{\Theta}(t) \times \mathbf{e}(t) \quad (2)$$

for the translational and rotational motion of the position \mathbf{r} and the orientation \mathbf{e} in two or three dimensions (2D, 3D). The active force is $\mathbf{F}^a = \gamma_T v_0 \mathbf{e}$, with v_0 the self-propulsion velocity and γ_T the translational friction coefficient; \mathbf{F} accounts for all non-active external forces, $\boldsymbol{\Gamma}$ is the translational thermal noise, and $\boldsymbol{\Theta}$ the rotational noise. The latter are Gaussian and Markovian random processes with zero mean and the second moments

$$\langle \Gamma_\alpha(t) \Gamma_\beta(t') \rangle = 2k_B T \gamma_T \delta_{\alpha\beta} \delta(t - t'), \quad (3)$$

$$\langle \Theta_\alpha(t) \Theta_\beta(t') \rangle = 2D_R \delta_{\alpha\beta} \delta(t - t'), \quad (4)$$

with k_B the Boltzmann factor, T the temperature, D_R the rotational diffusion coefficient, and $\alpha, \beta \in \{x, y, z\}$. Equation (2) yields the correlation function

$$\langle \mathbf{e}(t) \cdot \mathbf{e}(0) \rangle = e^{-(d-1)D_R t} \quad (5)$$

in d dimensions. Hence, the particle [Eq. (1)] can be considered as exposed to thermal and colored noise with the correlation function (5).

B. Active dumbbells and rods

The combination of active monomers into linear assemblies provides a wide spectrum of possible combinations of active forces. This is illustrated for two bound active particles forming a dumbbell. A bond, not restricting the orientational motion of two ABPs, leads to an active Brownian dumbbell. The dynamical properties and the phase behavior of such dumbbells have been studied.^{104,105} Since active dumbbells are a special case of active Brownian polymers, we refer to the general discussion is Sec. III for results. Specific features by hydrodynamic interactions are addressed in Sec. VI A.

Another extreme case is propulsion along the bond vector only. The equations of motion of the monomers for a

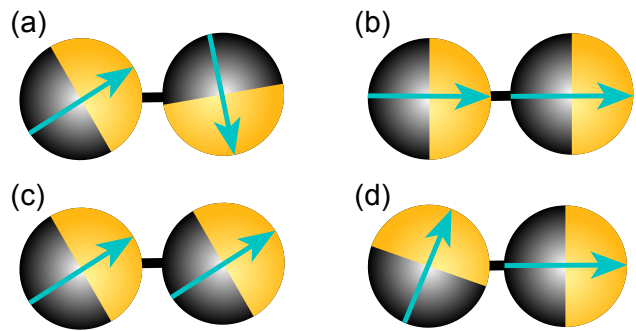


FIG. 1. Illustration of possible combinations of propulsion directions of active dumbbells. (a) The two ABPs rotate independently,^{104,105} (b) the beads are propelled along the bond,¹⁰⁶ (c) correlated propulsion in a common direction oblique to the bond, where the propulsion direction may change in a diffusive manner,¹⁰⁵ and (d) propulsion in non-parallel directions with fixed angles.¹⁰⁷

such a dumbbell are $(i \in \{1, 2\})$ ¹⁰⁶

$$\gamma_T \dot{\mathbf{r}}_i = \mathbf{F}^a(t) + \mathbf{F}_i(t) + \boldsymbol{\Gamma}_i(t), \quad (6)$$

with the active force $\mathbf{F}^a = F^a \mathbf{u}$ on every monomer in the direction of the (unit) bond vector $\mathbf{u} = (\mathbf{r}_2 - \mathbf{r}_1) / |\mathbf{r}_2 - \mathbf{r}_1|$. Note that \mathbf{F}_i contains the bond force. In the absence of any external force, thermal noise leads to a rotational diffusive motion of \mathbf{u} .¹⁰⁸ A generalization allows the active force to vary within a certain angle with respect to the bond vector.¹⁰⁹ Oblique arrangement of the propulsion direction leads to spiral trajectories in two dimensions, as has been demonstrated for Janus particles.¹⁰⁷ Naturally many other options are possible, and may, in modeling, be chosen according to experimental needs.

As indicated, the particular propulsion mechanism leads to a distinct dynamics and also effects on the emergent collective behavior can be expected, e.g., motility-induced phase separation (MIPS). In fact, MIPS has been found for dumbbells propelled along their bond¹⁰⁶ as well as those propelled oblique with respect to the bond,¹⁰⁵ where spontaneously formed aggregates break chiral symmetry and rotate.¹⁰⁶ Such a rotation is also obtained for systems of self-propelled particles¹¹⁰ or rods¹¹¹ moving in two dimensions on circles as well as for bend rigid self-propelled filaments.¹¹²

We focus on uniform systems of active particles of the same size, not addressing effects appearing in systems of dumbbells with different radii with correspondingly asymmetric flow fields.^{70,113–115}

C. Self-propelled force-free and torque-free monomers in fluids

Synthetic and biological microswimmers are typically immersed in a fluid and hydrodynamic interactions (HI)

are an integral part of their propulsion. Self-propelled particles move autonomously, with no external force or torque applied, and hence the total force/torque of the swimmer on the fluid and vice versa vanishes.^{6,116} The flow field generated by the microswimmer can be represented in terms of a multipole expansion.^{117–121} The far field is dominated by the force dipole (FD), source dipole (SD), force quadrupole (FQ), source quadrupole (SQ), and rotlet dipole (RD) contributions.^{119,122}

In theory and simulations, such an expansion can be exploited to calculate the flow field of individual swimmers. Alternatively, the squirmer model can be applied, which was originally designed to model ciliated microswimmers.^{123–125} It is a rather generic model, which captures the essential swimming aspects and is nowadays applied to a broad class of microswimmers,^{125–132} ranging from diffusiophoretic particles to biological cells.¹³³

A linear arrangement of such monomers leads to an intricate coupling of their flow fields and novel emergent conformational and dynamical features.^{120,134,135}

1. Squirmers

A squirmer is an axisymmetric rigid colloid with a prescribed surface fluid (slip) velocity.^{123–125,136} For a purely tangential fluid displacement, the surface slip velocity of a sphere can be described as

$$\mathbf{v}^{sq} = \sum_{n=1}^{\infty} \frac{2}{n(n+1)} B_n \sin \vartheta P'_n(\cos \vartheta) \mathbf{e}_{\vartheta} \quad (7)$$

in terms of derivatives of the n -th order Legendre polynomial, $P_n(\cos \vartheta)$. Here, ϑ is the angle between the body-fixed propulsion direction \mathbf{e} and the considered point on the colloid surface with tangent vector \mathbf{e}_{ϑ} , and B_n is the amplitude of the respective mode. Typically only two modes are considered, i.e., $B_n = 0$ for $n \geq 3$.^{125,126,130} Explicitly, the leading contributions yield the slip velocity^{125,126,130}

$$\mathbf{v}^{sq} = B_1 \sin \vartheta (1 + \beta \cos \vartheta) \mathbf{e}_{\vartheta}. \quad (8)$$

The parameter $B_1 = 2v_0/3$ determines the swimming velocity and $\beta = B_2/B_1$ characterizes the nature of the swimmer, namely a pusher ($\beta < 0$), puller ($\beta > 0$), and neutral squirmer ($\beta = 0$), corresponding, e.g., to *E. coli*, *Chlamydomonas*, and *Volvox*, respectively. The far field of a squirmer is well described by the flow fields of a force dipole (FD), a source dipole (SD), and a source quadrupole (SQ).^{122,130} Various extensions to spheroidal squirmers have been proposed,^{130,137,138} where some allow for an analytical calculation of the flow field.¹³⁰

The propulsion direction is not affected by the squirmer flow field. In case of several squirmers, but in absence of thermal fluctuations, interference of their flow fields leads to particular hydrodynamic collective effects and structure formation.^{131,139,140} In simulation approaches, which account for thermal fluctuations, often

different structures are observed, and in dilute solution the propulsion orientational correlation function agrees with Eq. (5) with the diffusion coefficient determined by the fluid viscosity.¹³⁰

2. Non-axisymmetric swimmers

For a more general description and an extension to non-axisymmetric swimmers, the swimmer equations of motion can be expressed in terms of mobilities.^{120,141–144} Such an extension captures the many-body nature of the surface-force density in a suspension of many colloids,¹⁴⁴ whereas the original Stokes law applies to infinite dilution only. The center-of-mass translational velocity and the rotational frequency of a single force- and torque-free spherical particle in an unbounded fluid are

$$\dot{\mathbf{r}} = \mathbf{v}^a(t), \quad \dot{\boldsymbol{\omega}} = \boldsymbol{\Omega}^a(t), \quad (9)$$

where the active velocity and active torque are given by

$$\mathbf{v}^a = -\frac{1}{4\pi R^2} \oint \mathbf{v}^s(\mathbf{r}) d^2r, \quad (10)$$

$$\boldsymbol{\Omega}^a = -\frac{3}{8\pi R^2} \oint \mathbf{r} \times \mathbf{v}^s(\mathbf{r}) d^2r, \quad (11)$$

with the surface slip velocity \mathbf{v}^s , e.g., the squirmer velocity of Eq. (8).^{141,144} More general expressions for ellipsoidal particles are presented in Ref. 145. This is a rather obvious result, but it shows that a colloid translates and rotates independently in response to the active surface velocity. The case of linearly connected active spheres is discussed in Sec. VI B.

III. DRY ACTIVE BROWNIAN POLYMERS (D-ABPO)

The conformational and dynamical properties of dry (free-draining) active Brownian polymers, which will be denoted as D-ABPO, are typically studied analytically by the well-known Rouse model¹⁴⁶ of equilibrium polymer physics.^{147–150} However, the deficiencies of the model, in particular the extensibility of bonds in the standard formulation, leads to inadequate predictions of activity effects. In contrast, valuable quantitative predictions have been obtained by computer simulations^{88,151–155} and more adequate analytical models, which will be introduced in the following.^{88,153,155,156}

A. Discrete model of active polymers

Dry semiflexible active polymers can be modeled as a linear chain of N_m linked active Brownian particles, with their dynamics described by the overdamped equations of motion (1) and (2). The force \mathbf{F}_i on particle i ($i = 1, \dots, N_m$) includes bond, bending, and excluded-volume contributions.^{88,95,155} The two independent parameters

v_0 and D_R , characterizing activity, are combined in the dimensionless quantities^{88,155,157}

$$Pe = \frac{v_0}{lD_R}, \quad \Delta = \frac{D_T}{d_H^2 D_R}, \quad (12)$$

with l the equilibrium bond length. The Péclet number Pe compares the time for the reorientation of an ABP monomer with that for its translation with velocity v_0 over the monomer radius, and Δ is the ratio between the translational, $D_T = k_B T / 3\pi\eta d_H$, and rotational, D_R , diffusion coefficient of an individual monomer, where d_H denotes the monomer hydrodynamic diameter.^{88,95,155} For a tangent hard-sphere-type polymer, $d_H = l$ and $\Delta = 1/3$. In order to avoid artifacts in the polymer structures by activity, the force constant for the bond, κ_l , and that of the excluded-volume Lennard-Jones potential, ε , can be adjusted according to $\kappa_l l^2 / k_B T = (10 + 2Pe) \times 10^3$ and $\varepsilon / (k_B T Pe) = 1$ as a function of Pe . This ensures a finite bond length within 3% of the equilibrium value for a harmonic bond potential, and an activity-independent overlap between monomers.^{88,95,155}

B. Continuum model of active polymers

An analytical description of D-ABPO properties is achieved by a mean-field model for semiflexible polymers^{158–166} augmented by the active velocity $\mathbf{v}(s, t)$, which yields the Langevin equation^{155,156,167}

$$\frac{\partial}{\partial t} \mathbf{r}(s, t) = \mathbf{v}(s, t) + \frac{1}{\gamma} \left(2\lambda k_B T \frac{\partial^2}{\partial s^2} \mathbf{r}(s, t) - \epsilon k_B T \frac{\partial^4}{\partial s^4} \mathbf{r}(s, t) + \mathbf{\Gamma}(s, t) \right), \quad (13)$$

with suitable boundary conditions for the free ends of linear polymers^{155,164–166} or periodic boundary conditions for ring polymers.¹⁵⁶ Here, γ is the translational friction coefficient per unit length and $\epsilon = 3/4p$ for polymers in three dimensions,^{168–170} where p is related to the persistence length l_p via $p = 1/(2l_p)$.^{163,171} The terms with the second and fourth derivative in Eq. (13) account for the entropic degrees of freedom and bending elasticity, respectively. The Lagrangian multiplier λ is determined in a mean-field manner by the global constraint of a finite contour length, L ,^{155,163,165,171,172}

$$\int_{-L/2}^{L/2} \left\langle \left(\frac{\partial \mathbf{r}(s, t)}{\partial s} \right)^2 \right\rangle ds = L, \quad (14)$$

From Eq. (5), the correlation function of the velocity $\mathbf{v}(s, t)$ follows as

$$\langle \mathbf{v}(s, t) \cdot \mathbf{v}(s', t') \rangle = v_0^2 l e^{-\gamma_R(t-t')} \delta(s - s'), \quad (15)$$

with $\gamma_R = 2D_R$ the damping factor of the rotational motion. For the analytical solution, only the first and second moment of the distribution of the active velocity are needed.¹⁵⁵

Note that the parameter l in Eq. (15) defines the number of active sites L/l along the polymer.¹⁵⁵

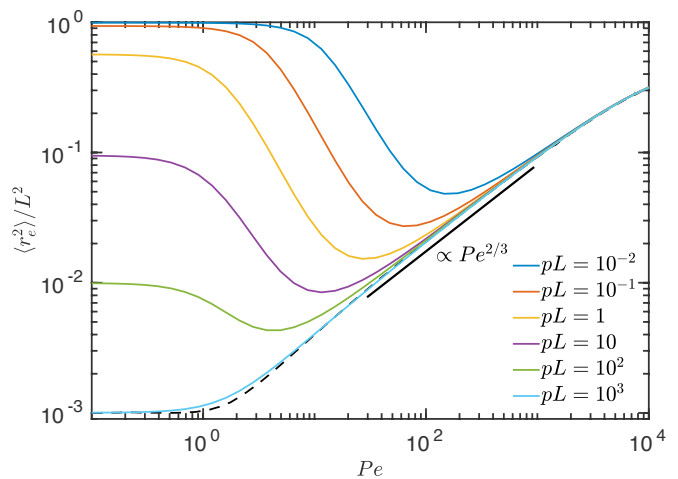


FIG. 2. Mean square end-to-end distances as a function of the Péclet number for semiflexible D-ABPO with $pL = L/2l_p = 10^3, 10^2, 10, 10^{-1}, 10^{-2}$ (bottom to top at $Pe = 10^{-1}$), and $\Delta = 1/3$.¹⁵⁵ The dashed line is the flexible polymer limit according to Eq. (18). “T. Eisenstecken, G. Gompper, and R. G. Winkler, *Polymers* **8**, 304 (2016); licensed under a Creative Commons Attribution (CC BY) license.”

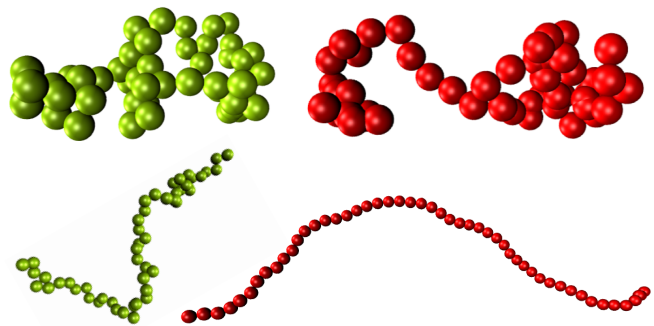


FIG. 3. Configurations of flexible phantom D-ABPO (red) and active polymers with self-propelled monomers in presence of HI (S-ABPO) (green) (cf. Sec. IV A) of length $N_m = 50$ for the Péclet numbers $Pe = 1$ (top) and $Pe = 10^3$ (bottom).⁸⁸ “Reproduced with permission from *Soft Matter* **12**, 8316 (2016). Copyright 2016 The Royal Society of Chemistry.”

C. Results

1. Conformational properties

The conformational properties of linear polymers are characterized by their mean square end-to-end distance¹⁵⁵

$$\langle r_e^2 \rangle = 4 \sum_{n=1}^{\infty} \langle \chi_{2n-1}^2 \rangle \varphi_{2n-1}^2(L/2), \quad (16)$$

in terms of the eigenfunctions φ_n of the differential operator on the rhs of Eq. (13) and the fluctuations of the normal-mode amplitudes

$$\langle \chi_n^2 \rangle = \frac{3k_B T}{\gamma} \tau_n + \frac{v_0^2}{p(1 + \gamma_R \tau_n)} \tau_n^2. \quad (17)$$

The relaxation times τ_n as well as the eigenfunctions depend on the activity. The closed expression

$$\langle r_e^2 \rangle = \frac{L}{p\mu} + \frac{Pe^2 L}{6p\mu\Delta} \left[1 - \frac{\sqrt{1 + 6\mu^2 \Delta}}{pL\sqrt{\mu}} \tanh \left(\frac{pL\sqrt{\mu}}{\sqrt{1 + 6\mu^2 \Delta}} \right) \right] \quad (18)$$

is obtained in the limit of flexible polymers, $pL \gg 1$, with free ends,¹⁵⁵ with the relaxation times

$$\tau_n = \frac{\tau_R}{\mu n^2}, \quad (19)$$

where $\tau_R = \gamma L^2 / (3\pi^2 k_B T p)$ is the (passive) Rouse relaxation time.^{146,164} The activity-dependent factor μ accounts for the constraint (14). A detailed discussion of $\mu(Pe)$ for linear and ring polymers is presented in Refs. 95, 155, and 156, respectively

The effect of activity on the conformational properties of active polymers is illustrated in Fig. 2. Figure 3 shows polymer conformations for various Péclet numbers. For flexible polymers, activity causes polymer swelling with increasing Pe , which saturates at $L^2/2$ in the limit $pL \rightarrow \infty$ as a consequence of the finite contour length. The reason for the swelling is an increase of the persistence length L_p of the active motion with increasing Pe , where L_p is defined as the distance displaced by activity with velocity v_0 in the time $1/2D_R$ of the decay of the correlation function (15), i.e., $L_p/l = Pe/2$. For $Pe \gg 1$, two groups of monomers moving in opposite directions will move far before changing their direction substantially, which leads to stretching of the in-between part of the polymer. In contrast, semiflexible polymers shrink at weak Pe and swell for large Pe similarly to flexible polymers. Shrinkage is caused by enhanced fluctuations transverse to the polymer contour by activity. The bonds prevent fluctuations along the contour, which leads to an apparent softening of the semiflexible polymer. At large Péclet numbers, tension in the polymer contour, which increases with activity, dominates over the energetic contribution of bending, so that the latter can be neglected and a semiflexible polymer appears flexible. The comparison of the theoretical predictions of the polymer conformations with simulation results yields excellent agreement.¹⁶⁷

In general, ring polymers exhibit similar features as linear polymers.¹⁵⁶ Specifically, active and thermal fluctuations attempt to shrink and crumple a ring-like structure. However, this is opposed by a negative internal tension, whereas the tension is always positive for linear polymers. In general, activity implies enhanced fluctuations of the normal-mode amplitudes.¹⁵⁶ The fluctuation

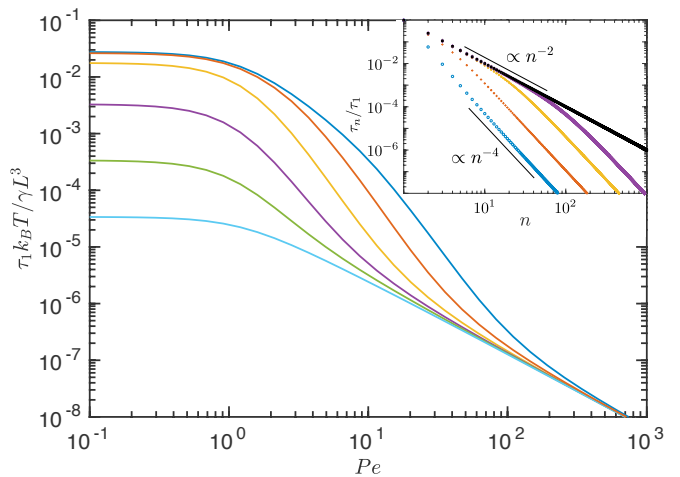


FIG. 4. Longest relaxation times of semiflexible D-ABPO as a function of the Péclet number for $pL = L/2lp = 10^3, 10^2, 10, 1, 10^{-1}$, and 10^{-2} (bottom to top). Inset: Mode-number dependence of the relaxation times of active polymers with $pL = 10^{-2}$ for the Péclet numbers $Pe = 10^1, 3 \times 10^1, 10^2$, and 5×10^2 (bottom to top). The black squares (top) show the mode-number dependence of flexible polymers with $pL = 10^3$. The solid lines indicate the relations for flexible ($\sim n^{-2}$) and semiflexible ($\sim (2n-1)^{-4}$) polymers, respectively. τ_1 is the longest relaxation time.¹⁵⁵ “T. Eisenstecken, G. Gompper, and R. G. Winkler, *Polymers* **8**, 304 (2016); licensed under a Creative Commons Attribution (CC BY) license.”

spectrum is dominated by activity already for moderate Péclet numbers ($Pe \gtrsim 10$)—the contribution with v_0^2 in Eq. (17)—and thermal fluctuations matter only for large mode numbers, i.e., at very small length scales. Notably, the major part of the spectrum is determined by tension, with a crossover from a $1/n^2$ to a $1/n^4$ power-law with increasing mode number (cf. Eq. (17) for $\tau_n \sim 1/n^2$). Hence, conclusions from the exponent on the underlying fluctuation mechanisms have to be drawn with care, and a $1/n^4$ dependence is not necessarily a sign of dominating bending modes.

Qualitatively, the obtained fluctuation spectrum for rings agrees with that of fluctuating membranes, where also an increase of the fluctuations at small wave vectors by activity compared to an equilibrium system has been observed experimentally,^{173–176} in simulations,^{174,175} and described theoretically.^{176,177}

2. Relaxation times

The polymer relaxation times strongly depend on the activity, as displayed in Fig. 4. The longest time, τ_1 , decreases with increasing Péclet number for $Pe \gtrsim 1$. According to Eq. (19), in the flexible limit, $\tau_1 \sim 1/\mu$ is solely determined by the stretching coefficient μ , and its decrease is a consequence of the finite polymer con-

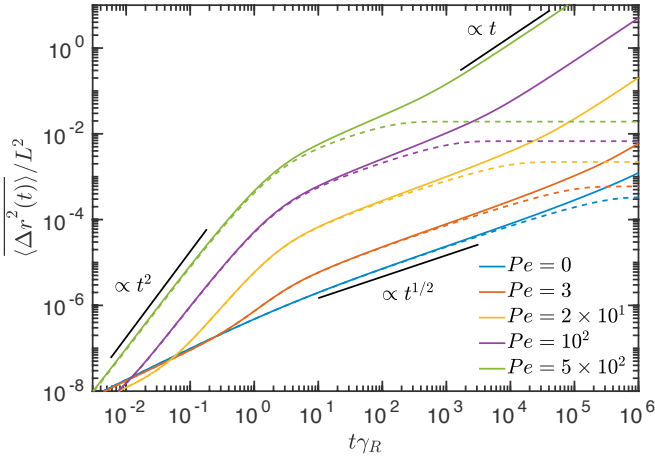


FIG. 5. Mean-square displacements (MSD) of flexible D-ABPO with $pL = 10^3$. The Péclet numbers are $Pe = 0, 3, 20, 10^2$, and 5×10^2 (bottom to top). The time is scaled by the factor $\gamma_R = 2D_R$ of the rotational diffusion. The dashed lines correspond to the MSD in the polymer center-of-mass reference frame.⁹⁵ “Reproduced from T. Eisenstecken, G. Gompfer, and R. G. Winkler, *J. Chem. Phys.* **146**, 154903 (2017), with the permission of AIP Publishing”

tour length. With increasing stiffness, the initial drop is stronger, but the same asymptotic dependence is obtained for $Pe \rightarrow \infty$.

The inset of Fig. 4 shows the dependence of the relaxation times τ_n of stiff polymers on the mode number. At low Pe , we find the well-known dependence $\tau_n/\tau_1 \sim (2n-1)^{-4}$ valid for semiflexible polymers.^{164,169,170} With increasing Pe , the ratio τ_n/τ_1 increases, and for $Pe \gtrsim 50$ the small-mode-number relaxation times exhibit the dependence $\tau_n/\tau_1 \sim n^{-2}$ of flexible polymers. At larger n , the relaxation times cross over to the semiflexible behavior again. However, the crossover point shifts to larger mode numbers with increasing activity. Hence, active polymers at large Péclet numbers appear flexible on large length and long time scales and only exhibit semiflexible behavior on small length scales.

The theoretically predicted dependence of τ_1 on Pe has not been directly confirmed by simulations yet. However, the very good quantitative agreement between theoretical and simulation results of polymer mean-square displacements⁹⁶ supports the reliability of the theoretically obtained activity dependence.

3. Mean-square displacement

The contour-length averaged mean-square displacement (MSD) of active polymers is⁹⁵

$$\begin{aligned} \overline{\langle \Delta \mathbf{r}^2(t) \rangle} &= \langle \Delta \mathbf{r}_{cm}^2(t) \rangle + \frac{1}{L} \sum_{n=1}^{\infty} \left[\frac{6k_B T \tau_n}{\gamma} (1 - e^{-t/\tau_n}) \right. \\ &\quad \left. + \frac{2v_0^2 l \tau_n^2}{1 + \gamma_R \tau_n} \left(1 - \frac{e^{-\gamma_R t} - \gamma_R \tau_n e^{-t/\tau_n}}{1 - \gamma_R \tau_n} \right) \right], \end{aligned} \quad (20)$$

with the center-of-mass mean-square displacement^{147,150,154,155}

$$\langle \Delta \mathbf{r}_{cm}^2(t) \rangle = \frac{6k_B T}{\gamma L} t + \frac{2v_0^2 l}{\gamma_R^2 L} (\gamma_R t - 1 + e^{-\gamma_R t}). \quad (21)$$

Equation (21) resembles the MSD of a single active Brownian particle, with a ballistic time regime for short times and a diffusive regime for long times (cf. Fig. 5) with the diffusion coefficient $D = k_B T [1 + 3Pe^2 / (2\Delta)] / (\gamma L)$.^{6,68,79,104} The polymer nature is reflected in the total friction coefficient γL , in the Brownian motion (first term on rhs of Eq. (21)), and the number of active sites L/l , in the active term.¹⁵⁵ The center-of-mass motion of polymers is free of internal forces, hence, the L/l ABPs contribute independently to the MSD. In the limit $t \rightarrow \infty$, the center-of-mass MSD is proportional to $v_0^2 l / L$. For an isotropic and homogeneous orientation of the propulsion directions, we expect no contribution of the active force to the MSD. However, by the Gaussian nature of the stochastic process, the orientation fluctuations are proportional to $\sqrt{l/L}$, which vanish in the limit $L \rightarrow \infty$, but lead to a finite contribution to the diffusion coefficient for $L < \infty$.

The site MSD (monomer MSD), cf. Fig. 5, is strongly affected by activity. It increases with increasing Pe , and exhibits up to four different time regimes.¹⁵⁵ In the limit $t \rightarrow 0$, the second term on the right hand side of Eq. (20) dominates and $\overline{\langle \Delta \mathbf{r}^2(t) \rangle} \sim (t/\tau_1)^{1/2}$, exhibiting Rouse dynamics, however, with activity-dependent relaxation time τ_1 . For $t/\tau_1 \ll 1$, $\gamma_R t \ll 1$, and $Pe \gg 1$, the active contribution dominates with a quadratic time dependence $\overline{\langle \Delta \mathbf{r}^2(t) \rangle} \sim t^2$. On time scales $1/\gamma_R \ll t \ll \tau_1$, the internal polymer dynamics is most important, with the Rouse-like time dependence $\overline{\langle \Delta \mathbf{r}^2(t) \rangle} \sim \gamma_R Pe^2 (\tau_1 t)^{1/2}$ in the center-of-mass reference frame. Since τ_1 decrease with increasing activity, this regime shortens with increasing Pe . At longer times, the center-of-mass MSD (21) dominates.^{88,155}

IV. WET ACTIVE BROWNIAN POLYMERS

Hydrodynamic interactions lead to a qualitative different polymer dynamics, as is well established for passive polymers,^{146,178} and first studies on active polymers

immersed in a fluid indicate even pronounced effects on their stationary-state conformational properties.^{88,96} The influence of hydrodynamics depends on the nature of the active force, i.e., self-propelled or bath-driven monomers.

Hydrodynamic interactions between monomers embedded in a fluid can be taken into account implicitly by the Oseen hydrodynamic tensor for point particles and the Rotne-Prager-Yamakawa (RPY) tensor for a sphere of diameter l .^{88,146,179–182}

Alternatively, hydrodynamics can explicitly be taken into account by mesoscale hydrodynamics simulation techniques, such as the lattice Boltzmann method (LB),^{183–186} the dissipative particle dynamics (DPD),^{187,188} and the multiparticle collision dynamics (MPC) approach.^{189–191} Externally driven active polymers have been implemented in MPC.⁸⁸

As mentioned above, the active, nonthermal process affecting the monomer dynamics can originate from internal sources or be imposed externally. In the first case, the monomer is force and torque free, whereas in the second case it is not. This leads to different equations of motion and consequently different behaviors.

A. Discrete model of self-propelled active polymers (S-ABPO)

For active polymers with self-propelled monomers (S-ABPO), the equations of motion are ($i = 1, \dots, N_m$)⁸⁸

$$\dot{\mathbf{r}}_i(t) = v_0 \mathbf{e}_i(t) + \sum_{j=1}^{N_m} \mathbf{H}_{ij} [\mathbf{F}_j(t) + \mathbf{J}_j(t)], \quad (22)$$

where \mathbf{F}_i comprises all inter- and intramolecular forces as for D-ABPO. The second moment of the Gaussian and Markovian random force is now given by

$$\langle \mathbf{F}_i(t) \mathbf{F}_j^T(t') \rangle = 2k_B T \mathbf{H}_{ij}^{-1} \delta(t - t'), \quad (23)$$

where \mathbf{H}_{ij}^{-1} is the inverse of the hydrodynamic tensor

$$\mathbf{H}_{ij}(\mathbf{r}_{ij}) = \frac{\delta_{ij}}{3\pi\eta l} \mathbf{I} + (1 - \delta_{ij}) \mathbf{G}(\mathbf{r}_{ij}), \quad (24)$$

and $\mathbf{G}(\mathbf{r})$ the Oseen or RPY tensor. The rotational motion of the monomers, Eq. (2), is not affected by hydrodynamics. No Stokeslet due to self-propulsion is taken into account, only Stokeslets arising from bond, bending, and excluded-volume interactions between monomers, as well as thermal forces are considered in this description. Higher-order multipole contributions of the active monomers are neglect, especially the force dipole. Since point particles are considered, source multipoles are absent. All these multipoles decay faster than a Stokeslet. Hence, the long-range character of HI in polymers of a broad class of active monomers are captured. As far as near-field hydrodynamic effects are concerned, this model is closest to polymers composed of

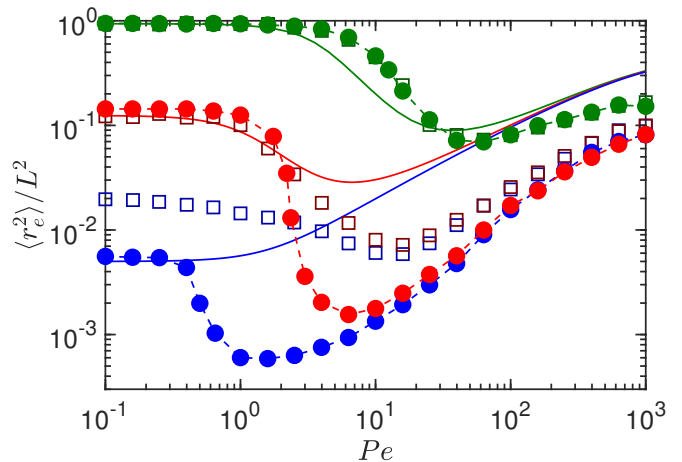


FIG. 6. Mean square end-to-end distance as a function of Péclet number for semiflexible S-ABPO with $N_m = 200$ ($L = 199l$) monomers for $pL = 2 \times 10^2$ (blue), 10^1 (red), and 10^{-1} (green). The bullets correspond to phantom and open squares to self-avoiding polymers. The dashed lines are guides for the eye.⁸⁸ The solid lines are analytical results for semiflexible free-draining polymers (D-ABPO). “Reproduced with permission from Soft Matter **12**, 8316 (2016). Copyright 2016 The Royal Society of Chemistry.”

neutral squirmers,^{126,127,192,193} where particular effects by higher multipole interactions between monomers are not resolved.^{120,134} Section VIA discusses orientational correlations of the propulsion directions of squirmer monomers of a dumbbell by higher-order multipoles.

The equations of motion (22) are solved by the ErmakMcCammon algorithm.^{194,195}

1. Conformational properties

Figure 6 depicts the conformations of the active polymers as a function of Pe , which are strongly influence by HI. Compared to free-draining polymers (D-ABPO), hydrodynamics leads to a substantial shrinkage of the polymers in the range $1 < Pe \lesssim 10^2$ and a reduced swelling for larger Pe . This qualitative difference is illustrated by the snapshots of Fig. 3. The shrinkage depends on polymer length and is substantially stronger for longer polymers.⁸⁸ Also semiflexible polymers in presence of HI shrink stronger than those in its absence, but the effect vanishes gradually as $pL \rightarrow 0$. This is a consequence of the reduced influence of hydrodynamic interactions for rather stiff polymers.¹⁷⁰ Yet, the asymptotic value for $Pe \rightarrow \infty$ is smaller than that for D-ABPO, because the conformational properties are determined by polymer entropy rather than stiffness in this limit, with a substantial hydrodynamic effect.

Self-avoidance reduces the extent of shrinkage, specifically for flexible polymers, but the excluded-volume effects vanish with decreasing pL , and for $pL < 1$ there is

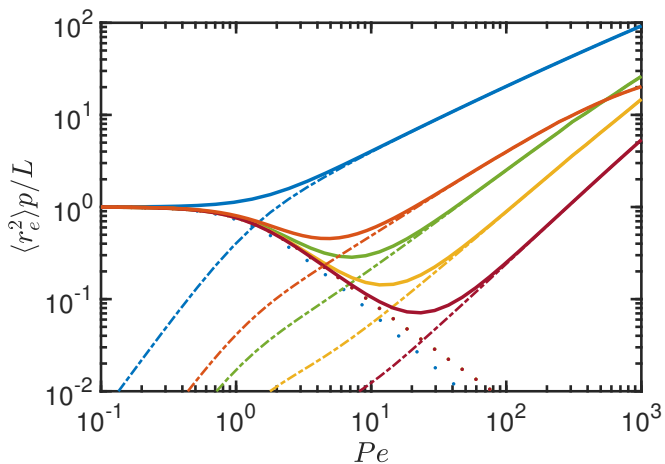


FIG. 7. Polymer mean square end-to-end distance $\langle r_e^2 \rangle$, Eq. (26), as a function of the Péclet number Pe for flexible S-ABPOs of length $pL = 2 \times 10^2$ (orange), 10^3 (green), 10^4 (yellow), and 10^5 (magenta). The blue lines correspond to a free-draining flexible polymers (D-ABPO) with $pL = 50$. The dotted curves represent the contribution with the relaxation times τ_n and the dashed-dotted curves that with v_0^2 of Eq. (26), respectively.⁸⁸ “Reproduced with permission from Soft Matter **12**, 8316 (2016). Copyright 2016 The Royal Society of Chemistry.”

hardly any difference between phantom and self-avoiding polymers. Moreover, the swelling behavior with and without excluded-volume interactions is rather similar in the limit $Pe \gg 1$. Interestingly, phantom and self-avoiding polymers show a different but universal dependence on Pe as they start to swell. Here, active forces exceed both, excluded-volume interactions and bending forces.

Analytical theory predicts a stronger increase of $\langle r_e^2 \rangle$ with increasing Pe in the swelling regime compared to D-ABPO (cf. Fig. 7). The dependence on Pe changes from $\langle r_e^2 \rangle \sim Pe$ for $pL \approx 10^2 - 10^3$ to $\langle r_e^2 \rangle \sim Pe^{3/2}$ for $pL \approx 10^5$. Hence, hydrodynamic interactions lead to a qualitative different Pe dependence.

The polymer collapse is a consequence of the time-scale separation of the thermal and the active contribution to the mean square end-to-end distance.⁸⁸ Hydrodynamic interactions enhance the polymer dynamics and shorten the relaxation times, as is well-known for the Zimm model of flexible polymers^{146,180,196} and also for semiflexible polymers.^{178,197,198} Within the preaveraging approximation,¹⁴⁶ the relaxation times are given by

$$\tilde{\tau}_n = \frac{\tau_n}{1 + 3\pi\eta G_{nn}}, \quad (25)$$

with τ_n the relaxation times in absence of hydrodynamic interactions, and G_{nn} the matrix elements of the Oseen tensor in terms of eigenfunctions of the semiflexible polymers.^{88,95,164} Since $G_{nn} \geq 0$, $\tilde{\tau}_n \leq \tau_n$. Analytical

theory yields the mean square end-to-end distance

$$\langle r_e^2 \rangle = \frac{8}{L} \sum_{n, \text{odd}} \left(\frac{k_B T \tau_n}{\pi \eta} + \frac{v_0^2 l \tilde{\tau}_n^2}{1 + \gamma_R \tilde{\tau}_n} \right), \quad (26)$$

where the first term in the brackets arises from thermal fluctuations and the second from activity. However, also the relaxation time τ_n and the elements G_{nn} depend on activity. Figure 7 displays the different contributions to $\langle r_e^2 \rangle$ for various polymer lengths. The initial shrinkage of $\langle r_e^2 \rangle$ with increasing Pe is caused by the decreasing relaxation times $\tau_n \sim 1/Pe$ with increasing activity.⁸⁸ The v_0^2 -dependent term causes a swelling of the polymers. For D-ABPO, the competing effects lead to an overall swelling, since swelling exceeds shrinkage. For S-ABPO, swelling is weaker due to fluid-induced collective motion compared to the random motion of D-ABPO, and $\langle r_e^2 \rangle$ assumes a minimum. This is a consequence of $\tilde{\tau}_n \leq \tau_n$.

Here, we like to mention that a certain amount of shrinkage has also been observed for self-avoiding D-ABPO over a certain range of Péclet numbers, which is attributed to specific monomer packing.^{167,199}

2. Dynamical properties

The mean-square displacement of flexible and semiflexible polymers exhibits the Zimm behavior $t^{2/3}$ or the dependence $t^{3/4}$ ($t/\tilde{\tau}_1 \ll 1$), respectively, for $Pe < 1$ in presence of hydrodynamic interactions.^{146,197,200} As for the D-ABPO, activity yields a ballistic time regime for $t/\tilde{\tau}_1 \ll 1$ and $\gamma_R t \ll 1$, and a regime dominated by internal polymer dynamics at times $1/\gamma_R \ll t \ll \tilde{\tau}_1$ for long polymers, $pL \gg 1$, and $Pe \gg 1$. Interestingly, in the latter regime analytical calculations yield the power-law behavior $\langle r_e^2 \rangle \sim t^{2/5}$, i.e., an exponent even smaller than that of D-ABPO.⁸⁸ For long times, $t/\tilde{\tau}_1 \gg 1$, the diffusive regime (21) of D-ABPO is assumed, with the same active diffusion coefficient.⁸⁸

B. Discrete model of externally actuated polymers (E-ABPO)

In case of externally actuated monomers (E-ABPO), the polymer equations of motion are given by⁹⁶

$$\dot{\mathbf{r}}_i(t) = \sum_{j=1}^{N_m} \mathbf{H}_{ij} [\gamma_T v_0 \mathbf{e}_j(t) + \mathbf{F}_j(t) + \mathbf{I}_j(t)]. \quad (27)$$

Here, also the external active force generates a Stokeslet for each monomer.

A possible realization of E-ABPO is a passive polymer embedded in an active bath. Experimentally, an externally driven polymer can in principle be realized by forcing a chain of colloidal particles by optical tweezers.²⁰¹ Optical forces are very well suited to manipulate objects as small as $5nm$ and up to hundreds of micrometers.²⁰¹

Combined with computer-generated holograms, many particles can be manipulated with a single laser beam at the same time.

1. Conformational properties

The mean square end-to-end distance of flexible E-ABPO increases monotonically with increasing Pe ,⁹⁶ in contrast to S-ABPO.⁸⁸ As for D-ABPO and S-ABPO, semiflexible polymers shrink initially with increasing Pe and swell again for large Péclet numbers in a universal manner. The comparison with the mean square end-to-end distance curves for D-ABPO reveals a stronger impact of activity on the conformations of E-ABPO. In particular, flexible polymers swell and semiflexible polymers shrink already for smaller Péclet numbers. However, the same asymptotic limit is assumed for $Pe \rightarrow \infty$, which follows from Eq. (28) for $\gamma_R \tilde{\tau}_n \ll 1$. Hence, S-ABPO exhibit the more compact structures compared to both, D-ABPO and E-ABPO. In the universal, stiffness- and excluded-volume-independent high- Pe regime, the mean square end-to-end distance exhibits the power-law increase $\langle r_e^2 \rangle \sim Pe^{1/2}$ with increasing Pe . This increase is weaker than that of D-ABPO, with the dependence $\langle r_e^2 \rangle \sim Pe^{2/3}$ (cf. Fig. 5), which emphasizes the strong effect of the internal dynamics on the active polymer conformational properties.⁹⁶

As for the shrinkage of the S-ABPO, enhanced swelling is related to a particular dependence of the mean square end-to-end distance on the relaxation times, which is given by

$$\langle r_e^2 \rangle = \frac{8}{L} \sum_{n, \text{odd}} \left(\frac{k_B T \tau_n}{\pi \eta} + \frac{v_0^2 l \tau_n^2}{1 + \gamma_R \tilde{\tau}_n} \right). \quad (28)$$

Since

$$\frac{\tau_n^2}{1 + \gamma_R \tilde{\tau}_n} \geq \frac{\tau_n^2}{1 + \gamma_R \tau_n} \geq \frac{\tilde{\tau}_n^2}{1 + \gamma_R \tilde{\tau}_n}, \quad (29)$$

the active contribution in Eq. (28) is larger than that of D-ABPO and S-ABPO, which implies a stronger overall swelling.⁹⁶

2. Dynamical properties

The distinct coupling between activity and hydrodynamics changes the activity-dependence of the relaxation times substantially, as illustrated in Fig. 8. Over a wide range of Péclet numbers, $\tilde{\tau}_1$ of E-ABPO is larger than the relaxation time of D-ABPO and S-ABPO, which is reflected in the strong increase of the mean square end-to-end distance. The (longest) relaxation time decreases with increasing Pe , hence, $\gamma_R \tilde{\tau}_n \ll 1$ in the limit $Pe \rightarrow \infty$. Moreover, $\tilde{\tau}_1$ exhibits the same dependence on Pe as τ_1 in absence of HI in that limit, which yields

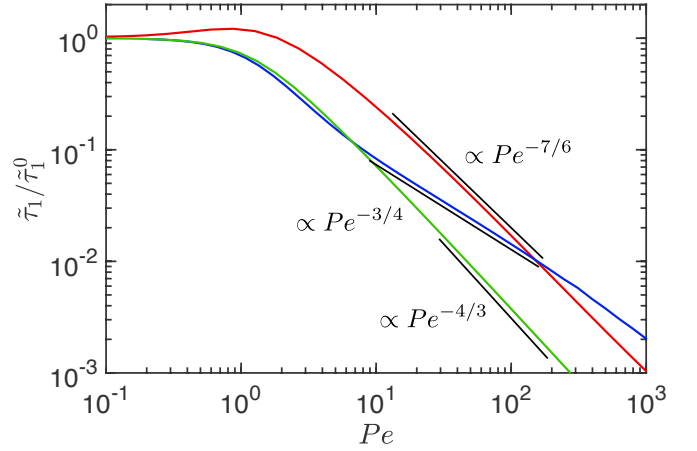


FIG. 8. Longest polymer relaxation time $\tilde{\tau}_1$ normalized by the corresponding passive value $\tilde{\tau}_1^0$ as a function of the Péclet number Pe for flexible D-ABPO (green), S-ABPO (blue), and E-ABPO (red) with $pL = 10^3$.

the same asymptotic value for $\langle r_e^2 \rangle$.⁹⁶ We like to emphasize that $\tilde{\tau}_1$ of semiflexible polymers assumes the same Pe dependence and scaling for $Pe \gg 1$ as flexible polymers (cf. Fig. 4).

The MSD exhibits the same sequence of time regimes as for D-ABPO and S-ABPO (cf. Fig. 5). Remarkably, long polymers exhibit a subdiffusive behavior for times $1/\gamma_R \ll t \ll \tilde{\tau}_1$ dominated by their internal dynamics, where analytical theory predicts the power-law time dependence $t^{5/7}$, which is close to $t^{3/4}$.

V. TANGENTIALLY DRIVEN FILAMENTS

Cytoskeleton polymers such as microtubules are rather stiff and are typically denoted as filaments. They exhibit active motion fueled by molecular motors *in vivo*²⁰² and *in vitro*.^{50,54–58,60,97,203–207} By the nature of their propulsion mechanism, such filaments are typically modeled as tangentially driven rodlike^{24,208–214} or semiflexible polymers^{93,109,112,134,215–222} in molecular approaches.

A. Continuum model

The theoretical description of Sec. III B can be adapted to the case of tangential driving semiflexible polymers, which yields the equation of motion

$$\begin{aligned} \gamma \frac{\partial}{\partial t} \mathbf{r}(s, t) &= f^a \frac{\partial}{\partial s} \mathbf{r}(s, t) \\ &+ 2\lambda k_B T \frac{\partial^2}{\partial s^2} \mathbf{r}(s, t) - \epsilon k_B T \frac{\partial^4}{\partial s^4} \mathbf{r}(s, t) + \mathbf{\Gamma}(s, t), \end{aligned} \quad (30)$$

with the active force f^a per unit length. This linear partial differential equation can be solved by an eigenfunction expansion in terms of the eigenfunctions $\psi_n(s)$ of

the equation $\mathcal{O}\psi_n(s) = -\xi_n\psi_n(s)$ with the operator

$$\mathcal{O} = f^a \frac{\partial}{\partial s} + 2\lambda k_B T \frac{\partial^2}{\partial s^2} - \epsilon k_B T \frac{\partial^4}{\partial s^4} \quad (31)$$

and the eigenvalues ξ_n . However, the operator \mathcal{O} is non-Hermitian, hence, an expansion into a biorthogonal basis set has to be applied, with the adjoint eigenvalue equation²²³ $\mathcal{O}^\dagger \psi_n^\dagger(s) = -\xi_n \psi_n^\dagger(s)$ and

$$\mathcal{O}^\dagger = -f^a \frac{\partial}{\partial s} + 2\lambda k_B T \frac{\partial^2}{\partial s^2} - \epsilon k_B T \frac{\partial^4}{\partial s^4}. \quad (32)$$

In case of a flexible polymers ($\epsilon = 0$), the eigenfunctions are²²⁴

$$\psi_n(s) = \sqrt{\frac{2}{L}} \frac{1}{\sqrt{k_n^2 + g^2}} e^{-gs} [k_n \cos(k_n s) + g \sin(k_n s)], \quad (33)$$

with $k_n = n\pi/L$, $g = f^a/(4\lambda k_B T)$, and the eigenvalues $\xi_n = 2\lambda k_B T(k_n^2 + g^2)$ for the boundary condition $\partial \mathbf{r}/\partial s = 0$ at $s = 0, L$, which implies $\partial \psi_n/\partial s = 0$ at $s = 0, L$. The adjunct eigenfunctions are $\psi_n^\dagger(s) = e^{2gs}\psi_n(s)$, and obey the boundary condition $d\psi_n^\dagger(s)/ds - 2g\psi_n^\dagger(s) = 0$ at $s = 0, L$. The eigenfunction for the eigenvalue $\xi_0 = 0$ is $\psi_0 = (2g/(e^{2gL} - 1))^{1/2}$.²²⁴

B. Discrete model

The dynamics of discrete polar active filaments is described by Eq. (6), with bond, bending, and excluded-volume forces. However, for the active force on particle i , various nonequivalent representations have been applied. In most cases, the active force is assumed to be tangential to the chain at a monomer,¹⁰⁹

$$\mathbf{F}_i^a = f^a \frac{\mathbf{r}_{i+1} - \mathbf{r}_{i-1}}{|\mathbf{r}_{i+1} - \mathbf{r}_{i-1}|} = f^a \mathbf{t}_i, \quad (34)$$

with the unit tangent vector \mathbf{t}_i . Other simulation studies utilized push-pull type forces²¹⁸

$$\mathbf{F}_i^a = \frac{f^a}{l} [(\mathbf{r}_{i+1} - \mathbf{r}_i) + (\mathbf{r}_i - \mathbf{r}_{i-1})] = \frac{f^a}{l} (\mathbf{r}_{i+1} - \mathbf{r}_{i-1}), \quad (35)$$

or^{216,220,221}

$$\mathbf{F}_i^a = f^a \left[\frac{\mathbf{r}_{i+1} - \mathbf{r}_i}{|\mathbf{r}_{i+1} - \mathbf{r}_i|} + \frac{\mathbf{r}_i - \mathbf{r}_{i-1}}{|\mathbf{r}_i - \mathbf{r}_{i-1}|} \right]. \quad (36)$$

For strong bond potentials and small bond-length variations, the latter two variants are essentially identical, but differ from Eq. (34). All these forces yield the same continuum limit (Eq. 30). In simulations, we can expect results to be independent of the adopted discretization for not too strong activities. However, deviations will emerge above a certain activity and, in particular, for a small number of monomers. This is reflected by the differences in the conformational properties of the continuous filaments (Eq. (30))²²² and of discrete models (cf. Sec. V C).^{109,221}

C. Results

The theoretical analysis of Sec. V A suggest that the conformational properties of flexible polar polymers are unaffected by activity. In particular, the mean square end-to-end distance is equal to the value of the passive counterpart.^{222,224} This is in contrast to simulation results for a discrete model, which indicate a shrinkage of flexible polymers at large active forces f^a ,^{109,221} for both, the active forces (34) as well as (36), although shrinkage is more pronounced for the force (34). The difference is a consequence of the particular discrete representation of the continuous polymers (cf. Sec. V B).

So far, very little further analytical results for individual polar filaments have been derived, specifically for semiflexible polymers, which might be related to the non-Hermitian character of the equations of motion.

Confinement in two dimensions enhances the influence of excluded-volume interactions on the emerging structures. Here, semiflexible filaments exhibit a transition to a spiral phase with increasing activity at $Pe \sim l_p/L$.^{218-220,225} Tethered filaments start beating in the presence of a polar force, or assume spiral shapes when the fixed end is able to rotate freely.^{217,226}

The filament dynamics depends on the composition of its ends. As an example, a load at the leading end leads to distinct locomotion patterns such as beating and rotation, depending on stiffness and propulsion strength.²²⁵

Simulations predict a substantial influence of hydrodynamic interactions on the rotational dynamics of single and multiple filaments as well on their collective dynamics and structure formation in 3D.^{216,227} According to the definition of Sec. IV B, the latter polymers are externally actuated by a tangential force of the type of Eq. (36).

VI. POLYMERS WITH SELF-PROPELLED COLLOIDAL MONOMERS

Polymers can be composed of monomers with their self-propulsion modeled by the concepts described in Sec. II C, i.e., as squirmers or a more general expansion of the monomer flow field. Although various studies have already been performed based on mobilities,^{120,144} only squirmer dumbbells have been considered so far. In contrast to the Brownian monomers of Secs. III and IV, the hydrodynamically self-propelled monomers include higher order multipoles such as force dipole, source dipole, etc.,^{122,130} which, by monomer-monomer interactions, give rise to additional features.

A. Linear squirmer assemblies

The swimming behavior of athermal squirmer dumbbells has been investigated by the boundary integral method,²²⁹ where, in this context, swimming refers to ballistic motion. The calculations show a strong effect of

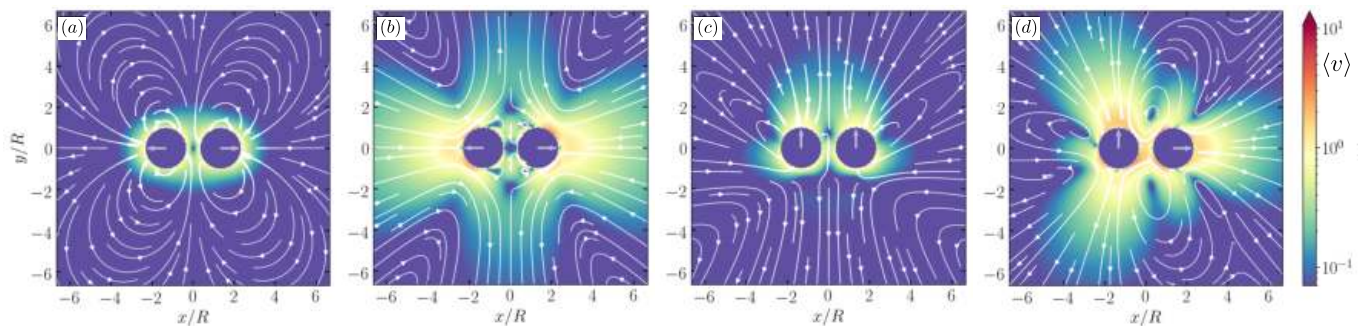


FIG. 9. Illustration of the flow field of a dumbbell composed of two spherical squirmers for their preferred propulsion directions. For (a) neutral squirmers ($\beta = 0$) and (b) pullers ($\beta = 5$), the propulsion direction is preferentially antiparallel. In the case of (c) a weak pusher ($\beta = -1$), the squirmer propulsion direction is mostly parallel and orthogonal to the bond. Stronger pushers ($\beta = -5$) exhibit preferentially an arrangement as in (c) as well as an orthogonal arrangement as in (d). Note that the flow fields are superpositions of the flow fields of the individual squirmers.²²⁸

the interfering swimmer flow fields on their orientation and locomotion. In particular, a flow-induced torque prevents stable forward swimming of individually freely rotating spherical squirmer in a dumbbell. By introducing a (short) bond, which restricts an independent rotation, circular trajectories for pushers and stable side-by-side swimming for pullers can be obtained.²²⁹

Athermal squirmer lack rotational diffusion, thus, absence of locomotion of freely rotating spheres in a dumbbell is a consequence of the missing thermal fluctuations of the fluid. Such fluctuations can be taken into account by mesoscale hydrodynamic simulations, e.g., the multiparticle collision dynamics (MPC) method,^{189–191} and locomotion is obtained. At infinite dilution, rotation is an activity-independent degree of freedom of a squirmer (cf. Sec. II C 1), which, however, strongly affects its long-time diffusion behavior, in the same way as for an ABP (see Eq. (21) for comparison)

Simulations of squirmer dumbbells yield preferred orientations of the propulsion directions, \mathbf{e}_i , with respect to each other and the bond connecting their centers, as illustrated in the snapshots of Fig. 9.^{228,230} This preference can be quantified by the average relative orientation of the propulsion direction, i.e., $\langle \mathbf{e}_1 \cdot \mathbf{e}_2 \rangle$. As expected for the active stresses, in dumbbells of neutral squirmers, alignment is very weak, and only for high Pe a slightly negative value is obtained. Puller exhibit very strong orientational correlations, with a preferential antiparallel alignment (cf. Fig. 9 (a), (b)). Strong correlations are also present for pushers, however, with a parallel alignment of the \mathbf{e}_i orthogonal with respect to the bond between the squirmers (Fig. 9(c)), and a near orthogonal arrangement as show in Fig. 9(d).

The preference in orientation is reflected in the dumbbell dynamics. The locomotion of the pusher dumbbell is closest to the dynamics of an ABP, specifically for $\beta \approx -1$. Significant deviations to an ABP dumbbell appear for smaller and large β . In particular, the preferred antiparallel alignment for neutral squirmers and pullers

leads to a pronounced slow-down of the dumbbell dynamics with a rather abrupt change at $\beta \gtrsim 0$. Notably, the long-time diffusion coefficient of puller dumbbells at large active stresses, $\beta = 5$, is reduced by orders of magnitude compared to that of ABP dumbbells. This is inline with the theoretical studies,²²⁹ however, thermal fluctuations are responsible for a finite diffusion coefficient at long times.

Hydrodynamic interactions between the monomer flow fields strongly affect the conformational properties of squirmer polymers. Simulations of dodecamers yield strongest swelling for neutral squirmers, and essentially no swelling for pullers ($\beta = 5$), with a mean square end-to-end distance close to the passive value.

B. Active filaments of tangentially propelled monomers

1. Colloidal monomers

The translational and rotational motion of chains of linearly connected monomers can be described by a set of Langevin equations.¹²⁰ The equations are based on the integral solution of Stokes flow,¹¹⁸ which is evaluated analytically by an expansion of the boundary fields in tensorial spherical harmonics. The omission of hydrodynamic many-body effects by the assumption of pair-wise additivity yields a computationally tractable approximation in terms of the Oseen tensor and its derivatives.²³¹ For tangentially driven filaments, the orientation of a monomer is no longer a dynamical degree of freedom, and the equations of motion reduce to translation only.

In contrast to the Brownian semiflexible polymers and filaments of Secs. III, IV, and V, where activity originates from an active velocity or force, the presence of higher order hydrodynamic multipoles yields active motion even in absence of a propulsion velocity. This is due to the generation of flows perpendicular to the tangent vector for a curved contour (cf. Fig. 10) This gives rise to partic-

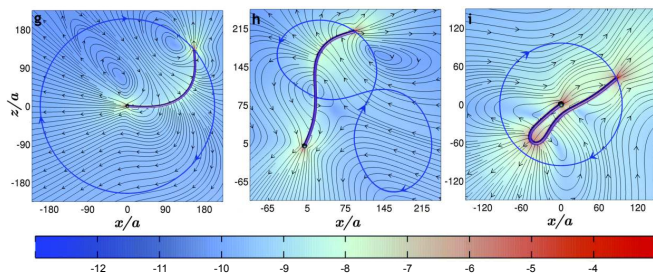


FIG. 10. Nonequilibrium stationary states of a single-end tethered filament. Increasing activity (from left to right) leads to particular stationary-state conformations and rotation (g, i), or filament beating (h). The background color indicates the logarithm of the magnitude of the fluid velocity. Reproduced from Ref. 120 with permission from the Royal Society of Chemistry. “Reproduced with permission from *Soft Matter* **11**, 9073 (2015). Copyright 2015 The Royal Society of Chemistry.”

ular stationary-state filament conformations and dynamical states, such as rotation of free filaments or beating and rotation of tethered filaments (cf. Fig. 10).^{120,134,135} Thermal noise will modify this behavior, to an extent which remains to be investigated.

2. Pointlike monomers

A somewhat simpler approach for hydrodynamically self-propelled, pointlike “monomers” has been suggested,²³² where Eq. (1) is employed for the monomer dynamics, however, with constraint rather than harmonic bond forces, and the force-dipole-type active force for a bond/link \mathbf{u}_{i+1} ,⁶

$$\mathbf{F}_i^a = -F_0 \mathbf{u}_{i+1}, \quad \mathbf{F}_{i+1}^a = F_0 \mathbf{u}_{i+1}, \quad (37)$$

where F_0 is magnitude of the force, and its sign implies extensile ($F_0 > 0$) or contractile ($F_0 < 0$) dipoles. The active forces are assumed to arise from stresses exerted by molecular motors temporarily attached to a bond. The time interval of the attached and detached states are taken from an exponential distribution.²³² The active velocity in the attached state is then

$$\mathbf{v}_i^a = \sum_j \mathbf{G}(\mathbf{r}_i - \mathbf{r}_j) \mathbf{F}_j^a(t). \quad (38)$$

Considering a single, long, and densely packed polymer in a spherical cavity, simulations show that hydrodynamic interactions between extensile dipoles can lead to large-scale coherent motion (cf. Sec. VII).

VII. COLLECTIVE BEHAVIOR

Already ABPs and active dumbbells exhibit an intriguing collective behavior, especially motility-induced phase

separation.^{39,79,99–101,105,106,132,233–237} Steric interactions by the extended shape of filaments and polymers, and their conformational degrees of freedom lead to further novel phenomena and behaviors.

Assays of microtubules mixed with molecular motors are paramount examples for collective effects emerging in out-of-equilibrium systems including polymers/filaments.^{58,60,97} Simplified systems comprising microtubules and kinesin motor constructs are able to self-organize into stable structures.⁵⁰ The motors dynamically crosslink the microtubules and their directed motion along the polar filaments leads to formation of vortex-like structures and asters with the microtubules arranged radially outward (Fig. 11(a)).⁵⁰ Along the same line, highly concentrated actin filaments propelled by molecular motors in a motility assay display emergent collective motion.^{56,206} Above a critical density, the filaments self-organize into coherently moving structures with persistent density modulations, such as clusters, swirls, and interconnected bands (Fig. 11(b)).⁵⁶ Furthermore, addition of a depletion agent to a concentrated microtubule-kinesin mixture leads to microtubule assemblance into bundles, hundreds of microns long.^{57,60,97} Kinesin clusters in bundles of microtubules of different polarity induce filament sliding and trigger their extension.⁶⁰ At high enough concentration, the microtubules form a percolating active network characterized by internally driven chaotic flows, hydrodynamic instabilities, enhanced transport, and fluid mixing.⁵⁷ Activity destroys long-range nematic ordering and leads to active turbulence, with short-range nematic order and dynamically creation and annihilation of topological defects (Fig. 11(c)).^{57,60}

The instability of the nematic phase of long polar filaments is usually attributed to the pusher-like hydrodynamics of systems with extensile force dipoles. A sinusoidal perturbation of the nematic order, with a wave vector along the filament direction, is amplified by the dipole flow field.²³⁸ However, a similar type of undulation instability is observed in simulations of semiflexible polar filaments, which are temporarily connected by motor proteins sliding them against each other—without any hydrodynamic interactions (cf. Fig. 12). This system is extensile, because motors mainly exert forces on antiparallel filaments. For an initially nematic phase with random filament orientation, first a polarity-sorting into bands occurs, followed by buckling of the bands, and a transition to an isotropic phase with polar domains (cf. Fig. 12).²³⁹ The isotropic phase is characterized by nematic-like $+1/2$ and $-1/2$ defects, as depicted in Fig. 11(c).⁵ Here, it is interesting to note that (i) active nematics are actually quite difficult to model on the filament level, because filaments move actively, but cannot have a preferred direction, and (ii) the filaments are actually *polar*, so that the system has both polar and nematic characteristics at the same time. This system has therefore been termed a *polar active nematic* in Ref. 239.

At surfaces, various flagellated bacteria alter their mor-

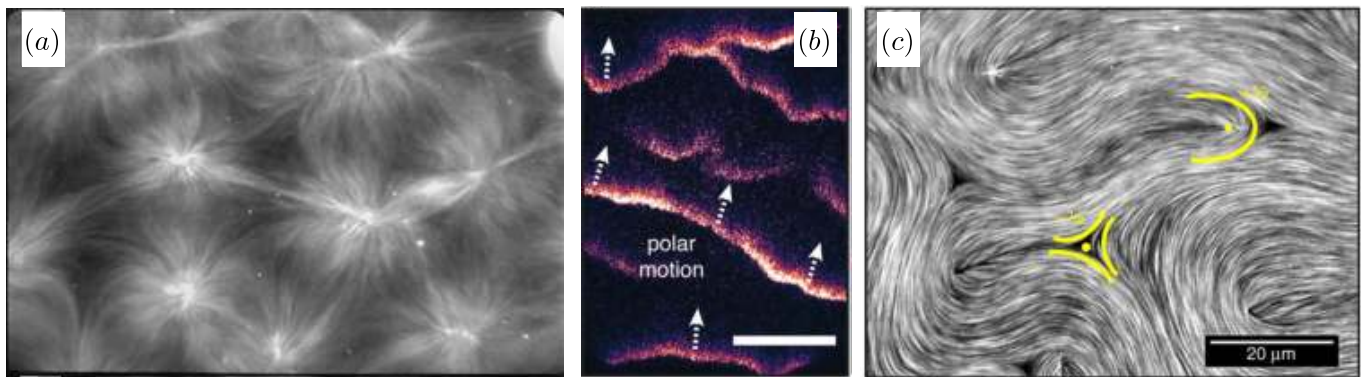


FIG. 11. Large-scale patterns formed by self-organization of biological filaments and molecular motors. (a) Lattice of asters and vortices formed by microtubules.⁵⁰ (b) Motility assay with fronts of polar actin clusters moving in the same direction as the filaments.²⁰⁶ (c) Network of nematically ordered microtubules exhibiting turbulent motion with a $+1/2$ (top right) and a $-1/2$ defect (bottom left).⁶⁰ (a) “Reproduced with permission from Nature **389**, 305 (1997). Copyright 1997 Macmillan Publishers Ltd.” (b) “Reproduced with permission from Science **361**, 255 (2018). Copyright 2018 AAAS.” (c) “A. Doostmohammadi, J. Ignés-Mullol, J. M. Yeomans, and F. Sagüés, Nat. Commun. **9**, 3246 (2018); licensed under a Creative Commons Attribution (CC BY) license.”

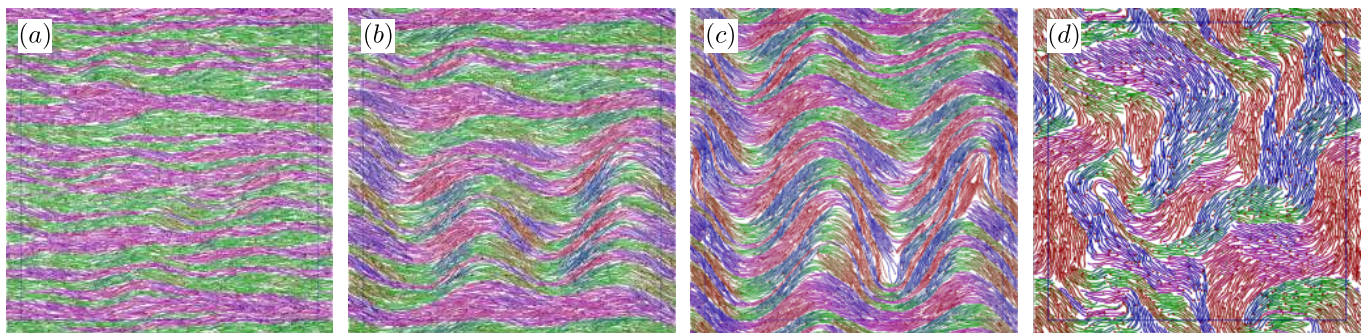


FIG. 12. Euler-like buckling instability of polar bands by semiflexible, propelled filaments. The snapshots depict a time sequence from (a) the development of polarity-sorted bands, (b), (c) progressive bending and breaking of bands, and finally (d) the formation of the long-time disordered structure.²³⁹ “G. Vliegenthart, A. Ravichandran, M. Ripoll, T. Auth, and G. Gompper, Sci. Adv. in press (2020); licensed under a Creative Commons Attribution (CC BY) license.”

phologies as they become more elongated by suppression of cell division. These so called swarmer cells migrate collectively over surfaces and are able to form stable aggregates, which can be highly motile (swarming).^{240,241} Some cells, such as *Proteus mirabilis* or *Vibrio parahaemolyticus* become rather elongated ($> 10 - 100 \mu\text{m}$) and polymer-like.⁴³ Since they are propelled by flagella, which are shorter than the body length and distributed all over the body, locomotion of individual cell is mainly tangential. Figure 13 shows that such cells can undergo large conformational changes from nearly rodlike to strongly bend structures while moving collectively in a film with other cells. As actin and microtubule filaments in dense suspensions, the swarmer cells exhibit local nematic order with defects and large-scale collective motion.

The collective effects of tangentially driven filaments have been studied by simulations in 2D, and new phases

depending on density, stiffness, activity, and aspect ratio have been identified.^{219,220} At moderate densities and activities, stiff filaments organize into mobile clusters, structures which are reminiscent to those formed by self-propelled rods.^{208–210,212–214} High activities and low bending rigidity yield spiral formation of individual filaments, which then translate as compact disc-like objects.²¹⁸ With increasing density, spiral collisions yield again motile clusters.²¹⁹ At moderate densities, a reentrant behavior is observed with increasing activity, from small clusters to giant clusters and back to small clusters.²¹⁹ Here, the disintegration of the giant cluster occurs when $Pe \sim l_p/L$, i.e. when active forces become comparable to bending forces. A similar threshold of $Pe \sim l_p/L$ is seen for the transition from open (equilibrium-polymer-like) conformations to spirals in the dilute case, due to the same force competition. At higher densities, a rich collective behavior is observed,

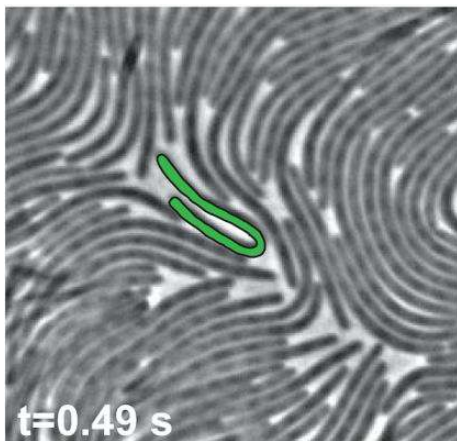


FIG. 13. Image of *P. mirabilis* swarmer cells in a colony actively moving across a surface.⁴³ The green, generally straight cell illustrates the ability of swarmer cells to bend substantially. “G. K. Auer, P. M. Oliver, M. Rajendram, T.-Y. Lin, Q. Yao, G. J. Jensen, and D. B. Weibel, *mBio* **10**, e00210 (2019); licensed under a Creative Commons Attribution (CC BY) license.”

such as a melt-like structures with topological defects.²²⁰ Even higher densities lead to jammed states of semiflexible filaments at small Péclet numbers, followed by laning and active turbulence for higher activities.²¹⁹ It is important to emphasize that this active turbulence occurs in a system without momentum conservation, and therefore at zero Reynolds number. Nevertheless, the turbulent state is characterized by a power-law decay of the kinetic-energy spectrum as a function of wave vector, reminiscent of Kolmogorov turbulence. The turbulent phase exhibits topological defects and a dynamics similar to the behavior seen theoretically in active nematics and experimentally in solutions of microtubules in presence of molecular motors.^{57,60,207}

A flexible polymer composed of hydrodynamically self-propelled, pointlike, and extensile force dipoles (cf. Sec. VIB 2), confined in a sphere, as a model of chromatin organized in the cell nucleus, shows large-scale coherent motion (cf. Fig. 15). The extensile force, mimicking a local molecular motor, reorganizes the polymer by stretching it into long and mutually aligned segments. This process is driven by the long-range flows generated along the chain by motor activity, which tends to both straighten the polymer locally and to align nearby regions.²³² As a result, large patches with high nematic order appear. Studies of passive and contractile polymers show that this transition to a highly coherent state is linked with the extensile dipole, which emphasizes the interplay between connectivity of dipoles in a chain and hydrodynamic interactions mediated by the embedding fluid.²³²

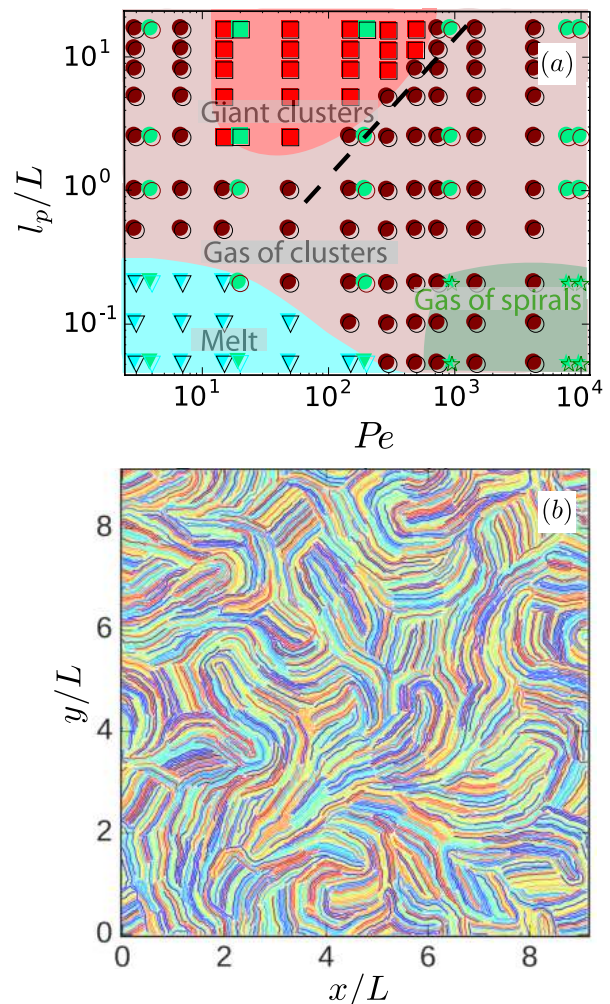


FIG. 14. (a) Phase diagram of tangentially driven semiflexible filaments as a function of $l_p/L = 1/(2pL)$ and Pe , where the Péclet number is defined as $Pe = f^a L^2 / (k_B T)$. Cyan triangles indicate the melt phase, magenta circles the gas of clusters, and the red squares the giant clusters phase. Green filled symbols depict the simulations with high aspect ratio filaments, $L/l = 100$, while the other points correspond to $L/l = 25$. (b) Snapshot of a high density turbulent phase at $Pe = 90$. The filament colors are chosen randomly.²¹⁹ “Reproduced with permission from *Soft Matter* **14**, 4483 (2018). Copyright 2018 The Royal Society of Chemistry.”

VIII. CONCLUSIONS AND OUTLOOK

We have demonstrated that the coupling of polymer degrees of freedom and active driving leads to many novel phenomena with respect to polymer conformational and dynamical properties. Depending on the nature of the active process—random vs. tangential driving—polymers swell or collapse, and their dynamics is typically enhanced. Moreover, hydrodynamic coupling of the flow field by the active monomeric units leads to long-range correlations and coherent motion. In ensem-

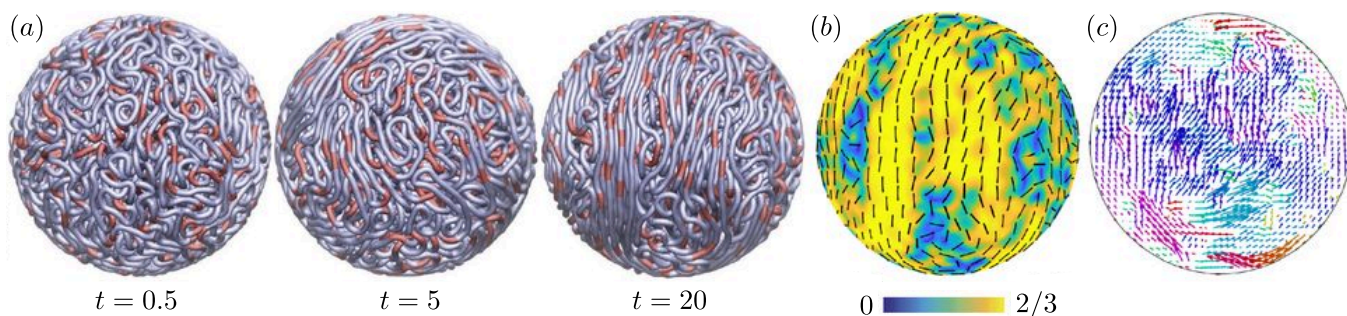


FIG. 15. Simulations of active chains with extensile dipoles. (a) Filament configurations at different times; the red segments indicate instantaneous dipole locations. (b) The nematic structure of the filaments in a shell adjacent to the surface of the confining sphere. The color code indicates the nematic order tensor. (c) Chromatin displacement map calculated in a plane across the spherical domain over a time interval $\Delta t = 0.2$. “Reproduced with permission from **115**, 1144263 (2018). Copyright 2018 National Academy of Sciences.”

bles of active polymers, steric and hydrodynamic interactions imply novel long-range collective turbulent motion with large-scale patterns. The various aspects emphasize the uniqueness of systems comprised of active polymers and filaments, and renders active soft matter a promising class of new materials.^{97,242}

We only begin to understand and to unravel the properties of polymeric active-matter systems. The current perspective article describes theoretical and modeling approaches and major results of mainly individual polymers and filaments. These approaches establish the basis for further studies in various directions.

Phase behavior—As mentioned, active particles and filaments exhibit novel collective phenomena and new phases such as MIPS. Typically two dimensional (2D) systems are considered, much less attention has been paid to three dimensional (3D) realizations. However, we can expect the appearance of novel structures and phases in 3D. First studies of active nematics consisting of microtubules and kinesin molecular motor yield a chaotic dynamics of the entire system.²⁴³ The analysis of spatial gradients of the director field show regions with large elastic distortions, which mainly form curvilinear structures as either isolated loops or belong to a complex network of system-spanning lines. These distortions are topological disclination lines characteristic of 3D nematics.²⁴³

Far less is known about the phase behavior of active Brownian polymers, both in 2D and 3D. Comparison of results for ABPs and active dumbbells in 2D indicate a shift of the critical activity for the onset of the MIPS to higher values.¹⁰⁵ We can expect a further shift of the critical point for longer polymers, and a possible suppression of the phase transition beyond a particular polymer length.

Confinement—Confinement will alter the properties of the active polymers substantially. Already spherical ABPs accumulate at walls. We expect an even stronger accumulation for active polymers. As an example, simulations of D-ABPO confined in a slit yield deviations

in the scaling behavior of the wall force established for passive polymers.²⁴⁴

Active-passive mixtures—New phenomena appear in mixtures of active and passive components. Already systems of ABPs mixed with passive colloids exhibit phase separation^{235,245,246} and a collective interface dynamics.²³⁵ Passive semiflexible polymers embedded in an active bath of ABPs exhibit novel transient states in 2D,^{151,247–249} where an activity-induced bending of the polymers implies an asymmetric exposure to active particles, with ABPs accumulating in regions of highest curvature, as has been observed for ABPs in confinement.²⁵⁰ This leads to particular polymer conformations such as hairpins, structures which are only temporarily stable and dissolve and rebuild in the course of time.

The presence of both active and passive components is a hallmark of living systems. So far, the impact of activity on the properties of the passive components is unclear. Simulations of two-component mixtures of polymers at different temperatures, which is an alternative approach to establish a nonequilibrium state,²⁵¹ yield phase separation of the two components.³⁶ Here, the two temperatures account for example for the activity of hetero- and euchromatin, which could play a role in chromatin separation in the cell nucleus.^{32–36} Although temperature control is an acceptable way of implementing activity differences, other out-of-equilibrium processes should be considered as well. Cells exhibit coherent structures—so-called membraneless organelles or condensates—encompassing and concentrating specific molecules such as proteins and RNA in the cytoplasm.^{252–254} *In-vivo* experiments suggest that active processes, which occur constantly within such organelles, play a role in their formation.^{252,253} An understanding of the interplay between equilibrium thermodynamic driving forces and nonequilibrium activity in organelle formation is fundamental in the strive to elucidate their functional properties, and their contribution to cell physiology and diseases.

Active-passive copolymers—Passive copolymer systems

self-assemble into ordered and tuneable structures in a wide range of morphologies, including spheres, cylinders, bicontinuous phases, lamellae, vesicles, and many other complex or hierarchical assemblies, driven by the preferred attractive and repulsive interactions between the different constituents of the copolymers.^{255,256} Copolymers composed of monomers of different activity will show an even richer phase and dynamical behavior, and will provide additional means to control structure formation and transport. Since biological macromolecules are rather intrinsically disorder than homogeneous, studies of copolymers will improve our understanding of structure formation in biological cells, for active polymers as well as for passive copolymers in an active bath. Specifically for polymeric assemblies of hydrodynamically self-propelled monomers, a strong hydrodynamical monomer-monomer coupling can be expected, e.g., by monomers with different active stress or diameter, leading to a rich dynamics and particular self-organized structures.¹¹⁵ Assembling several active/passive monomers into an unit may even be a route to design intelligent active particles, which sense and respond autonomously to other units and show swarm-intelligent behavior as schools of fish or swarms of birds.^{5,40,257,258}

Active turbulence—As mentioned several times, active nematics and bacteria exhibit chaotic, turbulent behavior. Up to now, similarities or differences to Kolmogorov-type turbulence²⁵⁹ of large Reynolds number fluids have not been resolved satisfactorily. In particular, the impact of polymer degrees of freedom needs to be investigated.

Hydrodynamic interactions—Various of the discussed examples highlight the relevance of hydrodynamic interactions for the conformational, dynamical, and collective effects of active polymers. Here, a broad range of studies are required to unravel hydrodynamics effects on the phase behavior of active polymers, their properties under confinement and under flow.

Rheology—Experiments show that the viscosity of a dilute suspension of swimming bacteria is lower than that of the fluid medium.^{260,261} This is a consequence of the interplay between bacteria (pushers) alignment with the flow and stress generation by the microswimmers, which enhances the applied shear stress and leads to an apparent viscosity reduction that increases with increasing volume fraction of cells.²⁶¹ Even “superfluidity” is obtained in bacterial suspensions at the onset of nonlinear flow and bacteria collective motion.^{260,261} Certainly, various of the observed aspects are of hydrodynamic origin and depend crucially on the flow field of the microswimmer. Analytical calculations of dilute dumbbell and D-ABPO systems already reveal an influence of activity on the zero-shear viscosity and on the shear thinning behavior.^{104,262} On a more macroscopic scale, shear experiments on long, slender, and entangled living worms (*Tubifex tubifex*) show that shear thinning is reduced by activity and the concentration dependence of the low-shear viscosity exhibits a different scaling from that of regular polymers.²⁶³ This highlights the wide range of rheological phenomena in ac-

tive matter. Clearly, systematic studies of various kinds of active polymers are needed to shed light onto their rheological behavior. Ultimately, such polymers might be useful as rheological modifiers.

In summary, there is a wide range of interesting aspects of active polymers, ranging from individual polymers with their different driving mechanisms, to their collective properties as a function of concentration, to rheological aspects. Simulations and analytical theories, which are based on the described models and approaches, will certainly play a decisive role in the elucidation of the many novel and unexpected nonequilibrium features of these systems.

DATA AVAILABILITY

The data that support the findings of this study are available from the corresponding author upon reasonable request.

ACKNOWLEDGMENTS

We thank C. Abaurrea-Velasco, T. Auth, J. Clopes, O. Duman, T. Eisenstecken, J. Elgeti, D. A. Fedosov, A. Ghavami, R. Isele-Holder, A. Martin Gomez, C. Philipps, A. Ravichandran, M. Ripoll, and G. A. Vliethart, for enjoyable collaborations and stimulating discussions. We gratefully acknowledge partial support from the DFG within the priority program SPP 1726 on Microswimmers—from Single Particle Motion to Collective Behaviour. A computing-time grant on the supercomputer JURECA at Jülich Supercomputing Centre (JSC) is thankfully acknowledged.

BIBLIOGRAPHY

- ¹Y. Demirel, “Nonequilibrium thermodynamics modeling of coupled biochemical cycles in living cells,” *J. Non-Newtonian Fluid Mech.* **165**, 953 (2010).
- ²X. Fang, K. Kruse, T. Lu, and J. Wang, “Nonequilibrium physics in biology,” *Rev. Mod. Phys.* **91**, 045004 (2019).
- ³R. Kapral, “Perspective: Nanomotors without moving parts that propel themselves in solution,” *J. Chem. Phys.* **138**, 020901 (2013).
- ⁴R. Kapral and A. S. Mikhailov, “Stirring a fluid at low Reynolds numbers: Hydrodynamic collective effects of active proteins in biological cells,” *Physica D* **318-319**, 100 (2016).
- ⁵M. C. Marchetti, J. F. Joanny, S. Ramaswamy, T. B. Liverpool, J. Prost, M. Rao, and R. A. Simha, “Hydrodynamics of soft active matter,” *Rev. Mod. Phys.* **85**, 1143 (2013).
- ⁶J. Elgeti, R. G. Winkler, and G. Gompper, “Physics of microswimmers—single particle motion and collective behavior: a review,” *Rep. Prog. Phys.* **78**, 056601 (2015).
- ⁷F. Jülicher, S. W. Grill, and G. Salbreux, “Hydrodynamic theory of active matter,” *Rep. Prog. Phys.* **81**, 076601 (2018).
- ⁸V. Hakim and P. Silberzan, “Collective cell migration: a physics perspective,” *Rep. Prog. Phys.* **80**, 076601 (2017).

- ⁹A. Be'er and G. Ariel, "A statistical physics view of swarming bacteria," *Mov. Ecol.* **7**, 9 (2019).
- ¹⁰A. Caspi, R. Granek, and M. Elbaum, "Enhanced diffusion in active intracellular transport," *Phys. Rev. Lett.* **85**, 5655 (2000).
- ¹¹A. W. C. Lau, B. D. Hoffman, A. Davies, J. C. Crocker, and T. C. Lubensky, "Microrheology, stress fluctuations, and active behavior of living cells," *Phys. Rev. Lett.* **91**, 198101 (2003).
- ¹²C. P. Brangwynne, G. H. Koenderink, F. C. MacKintosh, and D. A. Weitz, "Cytoplasmic diffusion: molecular motors mix it up," *J. Cell. Biol.* **183**, 583 (2008).
- ¹³D. Robert, T.-H. Nguyen, F. Gallet, and C. Wilhelm, "In vivo determination of fluctuating forces during endosome trafficking using a combination of active and passive microrheology," *PLOS ONE* **5**, e10046 (2010).
- ¹⁴N. Fakhri, A. D. Wessel, C. Willms, M. Pasquali, D. R. Klopstein, F. C. MacKintosh, and C. F. Schmidt, "High-resolution mapping of intracellular fluctuations using carbon nanotubes," *Science* **344**, 1031 (2014).
- ¹⁵M. Guo, A. J. Ehrlicher, M. H. Jensen, M. Renz, J. R. Moore, R. D. Goldman, J. Lippincott-Schwartz, F. C. Mackintosh, and D. A. Weitz, "Probing the stochastic, motor-driven properties of the cytoplasm using force spectrum microscopy," *Cell* **158**, 822 (2014).
- ¹⁶B. R. Parry, I. V. Surovtsev, M. T. Cabeen, C. S. O'Hern, E. R. Dufresne, and C. Jacobs-Wagner, "The bacterial cytoplasm has glass-like properties and is fluidized by metabolic activity," *Cell* **156**, 183 (2014).
- ¹⁷R. Golestanian, "Enhanced diffusion of enzymes that catalyze exothermic reactions," *Phys. Rev. Lett.* **115**, 108102 (2015).
- ¹⁸A. S. Mikhailov and R. Kapral, "Hydrodynamic collective effects of active protein machines in solution and lipid bilayers," *Proc. Natl. Acad. Sci. USA* **112**, E3639 (2015).
- ¹⁹S. C. Weber, A. J. Spakowitz, and J. A. Theriot, "Nonthermal ATP-dependent fluctuations contribute to the in vivo motion of chromosomal loci," *Proc. Natl. Acad. Sci. USA* **109**, 7338 (2012).
- ²⁰F. S. Gnesotto, F. Mura, J. Gladrow, and C. P. Broedersz, "Broken detailed balance and non-equilibrium dynamics in living systems: a review," *Rep. Prog. Phys.* **81**, 066601 (2018).
- ²¹F. Wu, A. Japaridze, X. Zheng, J. Wiktor, J. W. J. Kersemakers, and C. Dekker, "Direct imaging of the circular chromosome in a live bacterium," *Nat. Commun.* **10**, 2194 (2019).
- ²²F. C. MacKintosh and A. J. Levine, "Nonequilibrium mechanics and dynamics of motor-activated gels," *Phys. Rev. Lett.* **100**, 018104 (2008).
- ²³W. Lu, M. Winding, M. Lakonishok, J. Wildonger, and V. I. Gelfand, "Microtubule-microtubule sliding by kinesin-1 is essential for normal cytoplasmic streaming in *Drosophila* oocytes," *Proc. Natl. Acad. Sci. USA* **113**, E4995 (2016).
- ²⁴A. Ravichandran, G. A. Vliegthart, G. Saggiorato, T. Auth, and G. Gompper, "Enhanced dynamics of confined cytoskeletal filaments driven by asymmetric motors," *Biophys. J.* **113**, 1121 (2017).
- ²⁵C. A. Weber, R. Suzuki, V. Schaller, I. S. Aranson, A. R. Bausch, and E. Frey, "Random bursts determine dynamics of active filaments," *Proc. Natl. Acad. Sci. USA* **112**, 10703 (2015).
- ²⁶M. Guthold, X. Zhu, C. Rivetti, G. Yang, N. H. Thomson, S. Kasas, H. G. Hansma, B. Smith, P. K. Hansma, and C. Bustamante, "Direct observation of one-dimensional diffusion and transcription by *Escherichia coli* RNA polymerase," *Biophys. J.* **77**, 2284 (1999).
- ²⁷Y. X. Mejia, E. Nudler, and C. Bustamante, "Trigger loop folding determines transcription rate of *Escherichia coli*'s RNA polymerase," *Proc. Natl. Acad. Sci. USA* **112**, 743 (2015).
- ²⁸V. Belitsky and G. M. Schütz, "Stationary RNA polymerase fluctuations during transcription elongation," *Phys. Rev. E* **99**, 012405 (2019).
- ²⁹M. Di Pierro, D. A. Potoyan, P. G. Wolynes, and J. Onuchic, "Anomalous diffusion, spatial coherence, and viscoelasticity from the energy landscape of human chromosomes," *Proc. Natl. Acad. Sci. USA* **115**, 7753 (2018).
- ³⁰A. Javer, Z. Long, E. Nugent, M. Grisi, K. Siriawatwetchakul, K. D. Dorfman, P. Cicuti, and M. Cosentino Lagomarsino, "Short-time movement of *E. coli* chromosomal loci depends on coordinate and subcellular localization," *Nat. Commun.* **4**, 3003 (2013).
- ³¹A. Zidovska, D. A. Weitz, and T. J. Mitchison, "Micron-scale coherence in interphase chromatin dynamics," *Proc. Natl. Acad. Sci. USA* **110**, 15555 (2013).
- ³²E. Lieberman-Aiden, N. L. van Berkum, L. Williams, M. Imakaev, T. Ragozcy, A. Telling, I. Amit, B. R. Lajoie, P. J. Sabo, M. O. Dorschner, R. Sandstrom, B. Bernstein, M. A. Bender, M. Groudine, A. Gnirke, J. Stamatoyannopoulos, L. A. Mirny, E. S. Lander, and J. Dekker, "Comprehensive mapping of long-range interactions reveals folding principles of the human genome," *Science* **326**, 289 (2009).
- ³³T. Cremer, M. Cremer, B. Hübner, H. Strickfaden, D. Smeets, J. Popken, M. Sterr, Y. Markaki, K. Rippe, and C. Cremer, "The 4d nucleome: Evidence for a dynamic nuclear landscape based on co-aligned active and inactive nuclear compartments," *FEBS Lett.* **589**, 2931 (2015).
- ³⁴I. Solovei, K. Thanisch, and Y. Feodorova, "How to rule the nucleus: divide et impera," *Cell nucleus, Current Opinion in Cell Biology* **40**, 47 (2016).
- ³⁵N. Ganai, S. Sengupta, and G. I. Menon, "Chromosome positioning from activity-based segregation," *Nucleic Acids Res.* **42**, 4145 (2014).
- ³⁶J. Smrek and K. Kremer, "Small activity differences drive phase separation in active-passive polymer mixtures," *Phys. Rev. Lett.* **118**, 098002 (2017).
- ³⁷E. Lauga and T. R. Powers, "The hydrodynamics of swimming microorganisms," *Rep. Prog. Phys.* **72**, 096601 (2009).
- ³⁸S. Ramaswamy, "The mechanics and statistics of active matter," *Annu. Rev. Cond. Mat. Phys.* **1**, 323 (2010).
- ³⁹C. Bechinger, R. Di Leonardo, H. Löwen, C. Reichhardt, G. Volpe, and G. Volpe, "Active particles in complex and crowded environments," *Rev. Mod. Phys.* **88**, 045006 (2016).
- ⁴⁰G. Gompper, R. G. Winkler, T. Speck, A. Solon, C. Nardini, F. Peruani, H. Löwen, R. Golestanian, U. B. Kaupp, L. Alvarez, T. Kiørboe, E. Lauga, W. C. K. Poon, A. DeSimone, S. Muiños-Landin, A. Fischer, N. A. Söker, F. Cichos, R. Kapral, P. Gaspard, M. Ripoll, F. Sagues, A. Doostmohammadi, J. M. Yeomans, I. S. Aranson, C. Bechinger, H. Stark, C. K. Hemelrijk, F. J. Nedelec, T. Sarkar, T. Aryaksama, M. Lacroix, G. Duclos, V. Yashunsky, P. Silberzan, M. Arroyo, and S. Kale, "The 2020 motile active matter roadmap," *J. Phys: Condens. Matter* **32**, 193001 (2020).
- ⁴¹H. C. Berg, *E. Coli in Motion*, Biological and Medical Physics Series (Springer, New York, 2004).
- ⁴²WeibelLab, "Swarm timelapse," <https://www.youtube.com/watch?v=0YYAtPCIMc0> (August 3, 2012).
- ⁴³G. K. Auer, P. M. Oliver, M. Rajendram, T.-Y. Lin, Q. Yao, G. J. Jensen, and D. B. Weibel, "Bacterial swarming reduces *Proteus mirabilis* and *Vibrio parahaemolyticus* cell stiffness and increases β -lactam susceptibility," *mBio* **10**, e00210 (2019).
- ⁴⁴H. Li, X.-q. Shi, M. Huang, X. Chen, M. Xiao, C. Liu, H. Chaté, and H. P. Zhang, "Data-driven quantitative modeling of bacterial active nematics," *Proc. Natl. Acad. Sci. USA* **116**, 777 (2019).
- ⁴⁵M. H. Sohn, K. W. Seo, Y. S. Choi, S. J. Lee, Y. S. Kang, and Y. S. Kang, "Determination of the swimming trajectory and speed of chain-forming dinoflagellate *Cochlodinium polykrikoides* with digital holographic particle tracking velocimetry," *Mar. Biol. Biology* **158**, 561 (2011).
- ⁴⁶E. Selander, H. H. Jakobsen, F. Lombard, and T. Kiørboe, "Grazing cues induce stealth behavior in marine dinoflagellates," *Proc. Natl. Acad. Sci. USA* **108**, 4030 (2011).
- ⁴⁷Y. I. Yaman, E. Demir, R. Vetter, and A. Kocabas, "Emergence of active nematics in chaining bacterial biofilms," *Nat. Commun.*

- 10, 2285 (2019).
- ⁴⁸D. A. Gagnon and P. E. Arratia, “The cost of swimming in generalized newtonian fluids: experiments with *C. elegans*,” *J. Fluid Mech.* **800**, 753 (2016).
- ⁴⁹T. Sugi, H. Ito, M. Nishimura, and K. H. Nagai, “*C. elegans* collectively forms dynamical networks,” *Nat. Commun.* **10**, 683 (2019).
- ⁵⁰F. J. Nédélec, T. Surrey, A. C. Maggs, and S. Leibler, “Self-organization of microtubules and motors,” *Nature* **389**, 305 (1997).
- ⁵¹J. Howard, *Mechanics of motor proteins and the cytoskeleton* (Sinauer Associates Sunderland, MA, 2001).
- ⁵²K. Kruse, J. F. Joanny, F. Jülicher, J. Prost, and K. Sekimoto, “Asters, vortices, and rotating spirals in active gels of polar filaments,” *Phys. Rev. Lett.* **92**, 078101 (2004).
- ⁵³A. R. Bausch and K. Kroy, “A bottom-up approach to cell mechanics,” *Nat. Phys.* **2**, 231 (2006).
- ⁵⁴F. Jülicher, K. Kruse, J. Prost, and J.-F. Joanny, “Active behavior of the cytoskeleton,” *Phys. Rep.* **449**, 3 (2007).
- ⁵⁵Y. Harada, A. Noguchi, A. Kishino, and T. Yanagida, “Sliding movement of single actin filaments on one-headed myosin filaments,” *Nature* **326**, 805 (1987).
- ⁵⁶V. Schaller, C. Weber, C. Semmrich, E. Frey, and A. R. Bausch, “Polar patterns of driven filaments,” *Nature* **467**, 73 (2010).
- ⁵⁷T. Sanchez, D. T. N. Chen, S. J. DeCamp, M. Heymann, and Z. Dogic, “Spontaneous motion in hierarchically assembled active matter,” *Nature* **491**, 431 (2012).
- ⁵⁸Y. Sumino, K. H. Nagai, Y. Shitaka, D. Tanaka, K. Yoshikawa, H. Chate, and K. Oiwa, “Large-scale vortex lattice emerging from collectively moving microtubules,” *Nature* **483**, 448 (2012).
- ⁵⁹J. Prost, F. Jülicher, and J.-F. Joanny, “Active gel physics,” *Nat. Phys.* **11**, 111 (2015).
- ⁶⁰A. Doostmohammadi, J. Ignés-Mullol, J. M. Yeomans, and F. Sagués, “Active nematics,” *Nat. Commun.* **9**, 3246 (2018).
- ⁶¹J. C. Blain and J. W. Szostak, “Progress toward synthetic cells,” *Ann. Rev. Biochem.* **83**, 615 (2014).
- ⁶²P. Stano, “Is research on “synthetic cells” moving to the next level?” *Life* **9**, 3 (2018).
- ⁶³K. Göpflich, I. Platzman, and J. P. Spatz, “Mastering complexity: Towards bottom-up construction of multifunctional eukaryotic synthetic cells,” *Trends in Biotechnology* **36**, 938 (2018).
- ⁶⁴H. Löwen, “Active colloidal molecules,” *EPL* **121**, 58001 (2018).
- ⁶⁵R. G. Winkler, J. Elgeti, and G. Gompper, “Active polymers—emergent conformational and dynamical properties: A brief review,” *J. Phys. Soc. Jpn.* **86**, 101014 (2017).
- ⁶⁶G. Gompper, C. Bechinger, S. Herminghaus, R. Isele-Holder, U. B. Kaupp, H. Löwen, H. Stark, and R. G. Winkler, “Microswimmers—from single particle motion to collective behavior,” *Eur. Phys. J. Spec. Top.* **225**, 2061 (2016).
- ⁶⁷R. Niu and T. Palberg, “Modular approach to microswimming,” *Soft Matter* **14**, 7554 (2018).
- ⁶⁸J. R. Howse, R. A. L. Jones, A. J. Ryan, T. Gough, R. Vafabakhsh, and R. Golestanian, “Self-motile colloidal particles: From directed propulsion to random walk,” *Phys. Rev. Lett.* **99**, 048102 (2007).
- ⁶⁹H.-R. Jiang, N. Yoshinaga, and M. Sano, “Active motion of a janus particle by self-thermophoresis in a defocused laser beam,” *Physical Review Letters* **105**, 268302 (2010).
- ⁷⁰L. F. Valadares, Y.-G. Tao, N. S. Zacharia, V. Kitaev, F. Galembeck, R. Kapral, and G. A. Ozin, “Catalytic nanomotors: Self-propelled sphere dimers,” *Small* **6**, 565 (2010).
- ⁷¹A. Würger, “Thermal non-equilibrium transport in colloids,” *Rep. Prog. Phys.* **73**, 126601 (2010).
- ⁷²G. Volpe, I. Buttinoni, D. Vogt, H. J. Kümmerer, and C. Bechinger, “Microswimmers in patterned environments,” *Soft Matter* **7**, 8810 (2011).
- ⁷³S. Thutupalli, R. Seemann, and S. Herminghaus, “Swarming behavior of simple model squirmers,” *New J. Phys.* **13**, 073021 (2011).
- ⁷⁴I. Buttinoni, J. Bialké, F. Kümmel, H. Löwen, C. Bechinger, and T. Speck, “Dynamical clustering and phase separation in suspensions of self-propelled colloidal particles,” *Phys. Rev. Lett.* **110**, 238301 (2013).
- ⁷⁵B. ten Hagen, F. Kümmel, R. Wittkowski, D. Takagi, H. Löwen, and C. Bechinger, “Gravitaxis of asymmetric self-propelled colloidal particles,” *Nat. Commun.* **5**, 4829 (2014).
- ⁷⁶C. C. Maass, C. Krüger, S. Herminghaus, and C. Bahr, “Swimming droplets,” *Annu. Rev. Cond. Mat. Phys.* **7**, 171 (2016).
- ⁷⁷T. Vicsek and A. Zafeiris, “Collective motion,” *Phys. Rep.* **517**, 71 (2012).
- ⁷⁸P. Romanczuk, M. Bär, W. Ebeling, B. Lindner, and L. Schimansky-Geier, “Active Brownian particles,” *Eur. Phys. J. Spec. Top.* **202**, 1 (2012).
- ⁷⁹M. C. Marchetti, Y. Fily, S. Henkes, A. Patch, and D. Yllanes, “Minimal model of active colloids highlights the role of mechanical interactions in controlling the emergent behavior of active matter,” *Curr. Opin. Colloid Interface Sci.* **21**, 34 (2016).
- ⁸⁰A. Zöttl and H. Stark, “Emergent behavior in active colloids,” *J. Phys.: Condens. Matter* **28**, 253001 (2016).
- ⁸¹S. Ebbens, R. A. L. Jones, A. J. Ryan, R. Golestanian, and J. R. Howse, “Self-assembled autonomous runners and tumblers,” *Phys. Rev. E* **82**, 015304 (2010).
- ⁸²J. G. Gibbs, A. Nourhani, J. N. Johnson, and P. E. Lammert, “Spiral diffusion of self-assembled dimers of Janus spheres,” *MRS Adv.* **2**, 3471 (2017).
- ⁸³J. Yan, M. Han, J. Zhang, C. Xu, E. Luijten, and S. Granick, “Reconfiguring active particles by electrostatic imbalance,” *Nat. Mat.* **15**, 1095 (2016).
- ⁸⁴R. Di Leonardo, “Active colloids: Controlled collective motions,” *Nat. Mat.* **15**, 1057 (2016).
- ⁸⁵J. Zhang, J. Yan, and S. Granick, “Directed self-assembly pathways of active colloidal clusters,” *Angew. Chem. Int. Ed.* **55**, 5166 (2016).
- ⁸⁶J. Zhang and S. Granick, “Natural selection in the colloid world: active chiral spirals,” *Faraday Discuss.* **191**, 35 (2016).
- ⁸⁷D. Nishiguchi, J. Iwasawa, H.-R. Jiang, and M. Sano, “Flagellar dynamics of chains of active Janus particles fueled by an AC electric field,” *New. J. Phys.* **20**, 015002 (2018).
- ⁸⁸A. Martín-Gómez, T. Eisenstecken, G. Gompper, and R. G. Winkler, “Active Brownian filaments with hydrodynamic interactions: conformations and dynamics,” *Soft Matter* **15**, 3957 (2019).
- ⁸⁹H. R. Vutukuri, B. Bet, R. van Roij, M. Dijkstra, and W. T. S. Huck, “Rational design and dynamics of self-propelled colloidal bead chains: from rotators to flagella,” *Sci. Rep.* **7**, 16758 (2017).
- ⁹⁰Y. Sasaki, Y. Takikawa, V. S. R. Jampani, H. Hoshikawa, T. Seto, C. Bahr, S. Herminghaus, Y. Hidaka, and H. Orihara, “Colloidal caterpillars for cargo transportation,” *Soft Matter* **10**, 8813 (2014).
- ⁹¹F. Martínez-Pedrero, A. Ortiz-Ambriz, I. Pagonabarraga, and P. Tierno, “Colloidal microworms propelling via a cooperative hydrodynamic conveyor belt,” *Phys. Rev. Lett.* **115**, 138301 (2015).
- ⁹²G. Kokot, S. Das, R. G. Winkler, G. Gompper, I. S. Aranson, and A. Snezhko, “Active turbulence in a gas of self-assembled spinners,” *Proc. Natl. Acad. Sci. USA* **114**, 12870 (2017).
- ⁹³B. Biswas, R. K. Manna, A. Laskar, P. B. S. Kumar, R. Adhikari, and G. Kumaraswamy, “Linking catalyst-coated isotropic colloids into “active” flexible chains enhances their diffusivity,” *ACS Nano* **11**, 10025 (2017).
- ⁹⁴M. R. Shaebani, A. Wysocki, R. G. Winkler, G. Gompper, and H. Rieger, “Computational models for active matter,” *Nat. Rev. Phys.* **2**, 181 (2020).
- ⁹⁵T. Eisenstecken, G. Gompper, and R. G. Winkler, “Internal dynamics of semiflexible polymers with active noise,” *J. Chem. Phys.* **146**, 154903 (2017).
- ⁹⁶A. Martín-Gomez, T. Eisenstecken, G. Gompper, and R. G. Winkler, “Hydrodynamics of polymers in an active bath,” *Phys.*

- Rev. E* **101**, 052612 (2020).
- ⁹⁷D. Needleman and Z. Dogic, "Active matter at the interface between materials science and cell biology," *Nat. Rev. Mater.* **2**, 201748 (2017).
- ⁹⁸F. Peruani, L. Schimansky-Geier, and M. Bär, "Cluster dynamics and cluster size distributions in systems of self-propelled particles," *Eur. Phys. J. Spec. Top.* **191**, 173 (2010).
- ⁹⁹Y. Fily and M. C. Marchetti, "Athermal phase separation of self-propelled particles with no alignment," *Phys. Rev. Lett.* **108**, 235702 (2012).
- ¹⁰⁰J. Bialké, T. Speck, and H. Löwen, "Crystallization in a dense suspension of self-propelled particles," *Phys. Rev. Lett.* **108**, 168301 (2012).
- ¹⁰¹G. S. Redner, M. F. Hagan, and A. Baskaran, "Structure and dynamics of a phase-separating active colloidal fluid," *Phys. Rev. Lett.* **110**, 055701 (2013).
- ¹⁰²B. ten Hagen, R. Wittkowski, D. Takagi, F. Kümmel, C. Bechinger, and H. Löwen, "Can the self-propulsion of anisotropic microswimmers be described by using forces and torques?" *J. Phys.: Condens. Matter* **27**, 194110 (2015).
- ¹⁰³H. Löwen, "Inertial effects of self-propelled particles: From active Brownian to active Langevin motion," *J. Chem. Phys.* **152**, 040901 (2020).
- ¹⁰⁴R. G. Winkler, "Dynamics of flexible active Brownian dumbbells in the absence and the presence of shear flow," *Soft Matter* **12**, 3737 (2016).
- ¹⁰⁵J. T. Siebert, J. Letz, T. Speck, and P. Virnau, "Phase behavior of active Brownian disks, spheres, and dimers," *Soft Matter* **13**, 1020 (2017).
- ¹⁰⁶A. Suma, G. Gonnella, D. Marenduzzo, and E. Orlandini, "Motility-induced phase separation in an active dumbbell fluid," *EPL* **108**, 56004 (2014).
- ¹⁰⁷A. Nourhani, S. J. Ebbens, J. G. Gibbs, and P. E. Lammert, "Spiral diffusion of rotating self-propellers with stochastic perturbation," *Phys. Rev. E* **94**, 030601 (2016).
- ¹⁰⁸L. F. Cugliandolo, G. Gonnella, and A. Suma, "Rotational and translational diffusion in an interacting active dumbbell system," *Phys. Rev. E* **91**, 062124 (2015).
- ¹⁰⁹V. Bianco, E. Locatelli, and P. Malgaretti, "Globulelike conformation and enhanced diffusion of active polymers," *Phys. Rev. Lett.* **121**, 217802 (2018).
- ¹¹⁰Y. Yang, F. Qiu, and G. Gompper, "Self-organized vortices of circling self-propelled particles and curved active flagella," *Phys. Rev. E* **89**, 012720 (2014).
- ¹¹¹A. Kaiser and H. Löwen, "Vortex arrays as emergent collective phenomena for circle swimmers," *Phys. Rev. E* **87**, 032712 (2013).
- ¹¹²J. Denk, L. Huber, E. Reithmann, and E. Frey, "Active curved polymers form vortex patterns on membranes," *Phys. Rev. Lett.* **116**, 178301 (2016).
- ¹¹³Y.-G. Tao and R. Kapral, "Design of chemically propelled nanodimer motors," *J. Chem. Phys.* **128**, 164518 (2008).
- ¹¹⁴S. Michelin and E. Lauga, "Phoretic self-propulsion at finite Péclet numbers," *J. Fluid Mech.* **747**, 572 (2014).
- ¹¹⁵M. Wagner and M. Ripoll, "Hydrodynamic front-like swarming of phoretically active dimeric colloids," *EPL* **119**, 66007 (2017).
- ¹¹⁶R. G. Winkler and G. Gompper, "Hydrodynamics in motile active matter," *Handbook of Materials Modeling: Methods: Theory and Modeling*, *Handbook of Materials Modeling: Methods: Theory and Modeling*. Springer Handbook of Materials Modeling, 1 (2018).
- ¹¹⁷S. Kim and S. J. Karrila, *Microhydrodynamics: principles and selected applications* (Butterworth-Heinemann, Boston, 1991).
- ¹¹⁸C. Pozrikidis, *Boundary integral and singularity methods for linearized viscous flow* (Cambridge University Press, Cambridge, 1992).
- ¹¹⁹S. E. Spagnolie and E. Lauga, "Hydrodynamics of self-propulsion near a boundary: predictions and accuracy of far-field approximations," *J. Fluid Mech.* **700**, 105 (2012).
- ¹²⁰A. Laskar and R. Adhikari, "Brownian microhydrodynamics of active filaments," *Soft Matter* **11**, 9073 (2015).
- ¹²¹A. J. T. M. Mathijssen, A. Doostmohammadi, J. M. Yeomans, and T. N. Shendruk, "Hotspots of boundary accumulation: dynamics and statistics of micro-swimmers in flowing films," *J. R. Soc. Interface* **13**, 20150936 (2016).
- ¹²²R. G. Winkler and G. Gompper, "Hydrodynamics in motile active matter," in *Handbook of Materials Modeling: Methods: Theory and Modeling*, edited by W. Andreoni and S. Yip (Springer International Publishing, Cham, 2018) pp. 1–20.
- ¹²³M. J. Lighthill, "On the squirming motion of nearly spherical deformable bodies through liquids at very small Reynolds numbers," *Comm. Pure Appl. Math.* **5**, 109 (1952).
- ¹²⁴J. R. Blake, "A spherical envelope approach to ciliary propulsion," *J. Fluid Mech.* **46**, 199 (1971).
- ¹²⁵T. Ishikawa, M. P. Simmonds, and T. J. Pedley, "Hydrodynamic interaction of two swimming model micro-organisms," *J. Fluid Mech.* **568**, 119 (2006).
- ¹²⁶I. Llopis and I. Pagonabarraga, "Hydrodynamic interactions in squirmer motion: Swimming with a neighbour and close to a wall," *J. Non-Newtonian Fluid Mech.* **165**, 946 (2010).
- ¹²⁷I. O. Götze and G. Gompper, "Mesoscale simulations of hydrodynamic squirmer interactions," *Phys. Rev. E* **82**, 041921 (2010).
- ¹²⁸J. J. Molina, Y. Nakayama, and R. Yamamoto, "Hydrodynamic interactions of self-propelled swimmers," *Soft Matter* **9**, 4923 (2013).
- ¹²⁹A. Zöttl and H. Stark, "Hydrodynamics determines collective motion and phase behavior of active colloids in quasi-two-dimensional confinement," *Phys. Rev. Lett.* **112**, 118101 (2014).
- ¹³⁰M. Theers, E. Westphal, G. Gompper, and R. G. Winkler, "Modeling a spheroidal microswimmer and cooperative swimming in a narrow slit," *Soft Matter* **12**, 7372 (2016).
- ¹³¹N. Yoshinaga and T. B. Liverpool, "Hydrodynamic interactions in dense active suspensions: From polar order to dynamical clusters," *Phys. Rev. E* **96**, 020603 (2017).
- ¹³²M. Theers, E. Westphal, K. Qi, R. G. Winkler, and G. Gompper, "Clustering of microswimmers: interplay of shape and hydrodynamics," *Soft Matter* **14**, 8590 (2018).
- ¹³³M. N. Popescu, W. E. Uspal, Z. Eskandari, M. Tasinkevych, and S. Dietrich, "Effective squirmer models for self-phoretic chemically active spherical colloids," *Eur. Phys. J. E* **41**, 145 (2018).
- ¹³⁴G. Jayaraman, S. Ramachandran, S. Ghose, A. Laskar, M. S. Bhamla, P. B. S. Kumar, and R. Adhikari, "Autonomous motility of active filaments due to spontaneous flow-symmetry breaking," *Phys. Rev. Lett.* **109**, 158302 (2012).
- ¹³⁵A. Laskar, R. Singh, S. Ghose, G. Jayaraman, P. B. S. Kumar, and R. Adhikari, "Hydrodynamic instabilities provide a generic route to spontaneous biomimetic oscillations in chemomechanically active filaments," *Sci. Rep.* **3**, 1964 (2013).
- ¹³⁶T. J. Pedley, "Spherical squirmers: models for swimming micro-organisms," *IMA J. Appl. Math.* **81**, 488 (2016).
- ¹³⁷S. R. Keller and T. Y. Wu, "A porous prolate-spheroidal model for ciliated micro-organisms," *J. Fluid Mech.* **80**, 259 (1977).
- ¹³⁸K. Ishimoto and E. A. Gaffney, "Squirmer dynamics near a boundary," *Phys. Rev. E* **88**, 062702 (2013).
- ¹³⁹F. Alarcón and I. Pagonabarraga, "Spontaneous aggregation and global polar ordering in squirmer suspensions," *J. Mol. Liq.* **185**, 56 (2013).
- ¹⁴⁰F. Alarcón, C. Valeriani, and I. Pagonabarraga, "Morphology of clusters of attractive dry and wet self-propelled spherical particle suspensions," *Soft Matter* **13**, 814 (2017).
- ¹⁴¹R. Singh, S. Ghose, and R. Adhikari, "Many-body microhydrodynamics of colloidal particles with active boundary layers," *J. Stat. Mech. Theor. Exp.* **2015**, P06017 (2015).
- ¹⁴²B. U. Felderhof and R. B. Jones, "Small-amplitude swimming of a sphere," *Physica A* **202**, 119 (1994).
- ¹⁴³O. S. Pak and E. Lauga, "Generalized squirming motion of a sphere," *J. Eng. Math.* **88**, 1 (2014).

- ¹⁴⁴R. Singh and R. Adhikari, “Generalized stokes laws for active colloids and their applications,” *J. Phys. Commun.* **2**, 025025 (2018).
- ¹⁴⁵M. C. Fair and J. L. Anderson, “Electrophoresis of nonuniformly charged ellipsoidal particles,” *J. Colloid Interface Sci.* **127**, 388 (1989).
- ¹⁴⁶M. Doi and S. F. Edwards, *The Theory of Polymer Dynamics* (Clarendon Press, Oxford, 1986).
- ¹⁴⁷H. Vandebroek and C. Vanderzande, “Dynamics of a polymer in an active and viscoelastic bath,” *Phys. Rev. E* **92**, 060601 (2015).
- ¹⁴⁸D. Osmanovic and Y. Rabin, “Dynamics of active Rouse chains,” *Soft Matter* **13**, 963 (2017).
- ¹⁴⁹N. Samanta and R. Chakrabarti, “Chain reconfiguration in active noise,” *J. Phys. A: Math. Theor.* **49**, 195601 (2016).
- ¹⁵⁰S. Chaki and R. Chakrabarti, “Enhanced diffusion, swelling, and slow reconfiguration of a single chain in non-Gaussian active bath,” *J. Chem. Phys.* **150**, 094902 (2019).
- ¹⁵¹J. Harder, C. Valeriani, and A. Cacciuto, “Activity-induced collapse and reexpansion of rigid polymers,” *Phys. Rev. E* **90**, 062312 (2014).
- ¹⁵²D. Sarkar, S. Thakur, Y.-G. Tao, and R. Kapral, “Ring closure dynamics for a chemically active polymer,” *Soft Matter* **10**, 9577 (2014).
- ¹⁵³A. Ghosh and N. S. Gov, “Dynamics of active semiflexible polymers,” *Biophys. J.* **107**, 1065 (2014).
- ¹⁵⁴J. Shin, A. G. Cherstvy, W. K. Kim, and R. Metzler, “Facilitation of polymer looping and giant polymer diffusivity in crowded solutions of active particles,” *New J. Phys.* **17**, 113008 (2015).
- ¹⁵⁵T. Eisenstecken, G. Gompper, and R. G. Winkler, “Conformational properties of active semiflexible polymers,” *Polymers* **8**, 304 (2016).
- ¹⁵⁶S. M. Mousavi, G. Gompper, and R. G. Winkler, “Active Brownian ring polymers,” *J. Chem. Phys.* **150**, 064913 (2019).
- ¹⁵⁷S. Das, G. Gompper, and R. G. Winkler, “Confined active Brownian particles: theoretical description of propulsion-induced accumulation,” *New J. Phys.* **20**, 015001 (2018).
- ¹⁵⁸M. G. Bawendi and K. F. Freed, “A Wiener integral model for stiff polymer chains,” *J. Chem. Phys.* **83**, 2491 (1985).
- ¹⁵⁹S. M. Battacharjee and M. Muthukumar, “Statistical mechanics of solutions of semiflexible chains: A path integral formulation,” *J. Chem. Phys.* **86**, 411 (1987).
- ¹⁶⁰J. B. Langowski, J. Noolandi, and B. Nickel, “Stiff chain model—functional integral approach,” *J. Chem. Phys.* **95**, 1266 (1991).
- ¹⁶¹R. G. Winkler, P. Reineker, and L. Harnau, “Models and equilibrium properties of stiff molecular chains,” *J. Chem. Phys.* **101**, 8119 (1994).
- ¹⁶²B. Y. Ha and D. Thirumalai, “A mean-field model for semiflexible chains,” *J. Chem. Phys.* **103**, 9408 (1995).
- ¹⁶³R. G. Winkler, “Deformation of semiflexible chains,” *J. Chem. Phys.* **118**, 2919 (2003).
- ¹⁶⁴L. Harnau, R. G. Winkler, and P. Reineker, “Dynamic properties of molecular chains with variable stiffness,” *J. Chem. Phys.* **102**, 7750 (1995).
- ¹⁶⁵R. G. Winkler, “Conformational and rheological properties of semiflexible polymers in shear flow,” *J. Chem. Phys.* **133**, 164905 (2010).
- ¹⁶⁶R. G. Winkler, “Semiflexible polymers in shear flow,” *Phys. Rev. Lett.* **97**, 128301 (2006).
- ¹⁶⁷T. Eisenstecken, A. Ghavami, A. Mair, G. Gompper, and R. G. Winkler, “Conformational and dynamical properties of semiflexible polymers in the presence of active noise,” *AIP Conf. Proc.* **1871**, 050001 (2017).
- ¹⁶⁸O. Kratky and G. Porod, “Röntgenuntersuchung gelöster Fadenmoleküle,” *Recl. Trav. Chim. Pays-Bas* **68**, 1106 (1949).
- ¹⁶⁹S. R. Aragón and R. Pecora, “Dynamics of wormlike chains,” *Macromolecules* **18**, 1868 (1985).
- ¹⁷⁰R. G. Winkler, “Diffusion and segmental dynamics of rodlike molecules by fluorescence correlation spectroscopy,” *J. Chem. Phys.* **127**, 054904 (2007).
- ¹⁷¹R. G. Winkler and P. Reineker, “Finite size distribution and partition functions of Gaussian chains: Maximum entropy approach,” *Macromolecules* **25**, 6891 (1992).
- ¹⁷²R. G. Winkler, S. Keller, and J. O. Rädler, “Intramolecular dynamics of linear macromolecules by fluorescence correlation spectroscopy,” *Phys. Rev. E* **73**, 041919 (2006).
- ¹⁷³M. D. El Alaoui Faris, D. Lacoste, J. Pécéréaux, J. F. Joanny, J. Prost, and P. Bassereau, “Membrane tension lowering induced by protein activity,” *Phys. Rev. Lett.* **102**, 038102 (2009).
- ¹⁷⁴H. Turlier, D. A. Fedosov, B. Audoly, T. Auth, N. S. Gov, C. Sykes, J. F. Joanny, G. Gompper, and T. Betz, “Equilibrium physics breakdown reveals the active nature of red blood cell flickering,” *Nat. Phys.* **12**, 513 (2016).
- ¹⁷⁵H. R. Vutukuri, M. Hoore, C. Abaurrea-Velasco, L. van Buren, A. Dutto, T. Auth, D. A. Fedosov, G. Gompper, and J. Vermant, “Sculpting vesicles with active particles: Less is more,” *Nature*, in press (2020), [arXiv:1911.02381 \[cond-mat.soft\]](https://arxiv.org/abs/1911.02381).
- ¹⁷⁶S. C. Takatori and A. Sahu, “Active contact forces drive nonequilibrium fluctuations in membrane vesicles,” *Phys. Rev. Lett.* **124**, 158102 (2020).
- ¹⁷⁷B. Loubet, U. Seifert, and M. A. Lomholt, “Effective tension and fluctuations in active membranes,” *Phys. Rev. E* **85**, 031913 (2012).
- ¹⁷⁸L. Harnau, R. G. Winkler, and P. Reineker, “Dynamic structure factor of semiflexible macromolecules in dilute solution,” *J. Chem. Phys.* **104**, 6355 (1996).
- ¹⁷⁹J. Rotne and S. Prager, “Variational treatment of hydrodynamic interaction in polymers,” *J. Chem. Phys.* **50**, 4831 (1969).
- ¹⁸⁰H. Yamakawa, “Transport properties of polymer chains in dilute solution: Hydrodynamic interaction,” *J. Chem. Phys.* **53**, 436 (1970).
- ¹⁸¹A. Jain, P. Sunthar, B. Dünweg, and J. R. Prakash, “Optimization of a brownian-dynamics algorithm for semidilute polymer solutions,” *Phys. Rev. E* **85**, 066703 (2012).
- ¹⁸²J. K. G. Dhont, *An Introduction to Dynamics of Colloids* (Elsevier, Amsterdam, 1996).
- ¹⁸³G. R. McNamara and G. Zanetti, “Use of the Boltzmann equation to simulate lattice-gas automata,” *Phys. Rev. Lett.* **61**, 2332 (1988).
- ¹⁸⁴X. Shan and H. Chen, “Lattice Boltzmann model for simulating flows with multiple phases and components,” *Phys. Rev. E* **47**, 1815 (1993).
- ¹⁸⁵S. Succi, *The lattice Boltzmann equation: for fluid dynamics and beyond* (Oxford University Press, 2001).
- ¹⁸⁶B. Dünweg and A. C. Ladd, “Lattice Boltzmann simulations of soft matter systems,” *Adv. Polym. Sci.* **221**, 89 (2009).
- ¹⁸⁷P. J. Hoogerbrugge and J. M. V. A. Koelman, “Simulating microscopic hydrodynamics phenomena with dissipative particle dynamics,” *Europhys. Lett.* **19**, 155 (1992).
- ¹⁸⁸P. Español and P. B. Warren, “Statistical mechanics of dissipative particle dynamics,” *Europhys. Lett.* **30**, 191 (1995).
- ¹⁸⁹A. Malevanets and R. Kapral, “Mesoscopic model for solvent dynamics,” *J. Chem. Phys.* **110**, 8605 (1999).
- ¹⁹⁰R. Kapral, “Multiparticle collision dynamics: Simulations of complex systems on mesoscale,” *Adv. Chem. Phys.* **140**, 89 (2008).
- ¹⁹¹G. Gompper, T. Ihle, D. M. Kroll, and R. G. Winkler, “Multiparticle collision dynamics: A particle-based mesoscale simulation approach to the hydrodynamics of complex fluids,” *Adv. Polym. Sci.* **221**, 1 (2009).
- ¹⁹²M. Theers, E. Westphal, G. Gompper, and R. G. Winkler, “From local to hydrodynamic friction in Brownian motion: A multiparticle collision dynamics simulation study,” *Phys. Rev. E* **93**, 032604 (2016).
- ¹⁹³R. G. Winkler, “Low Reynolds number hydrodynamics and mesoscale simulations,” *Eur. Phys. J. Spec. Top.* **225**, 2079 (2016).
- ¹⁹⁴M. P. Allen and D. J. Tildesley, *Computer Simulation of Liquids* (Clarendon Press, Oxford, 1987).

- ¹⁹⁵D. L. Ermak and J. McCammon, “Brownian dynamics with hydrodynamic interactions,” *J. Chem. Phys.* **69**, 1352 (1978).
- ¹⁹⁶B. H. Zimm, “Dynamics of polymer molecules in dilute solution: Viscoelasticity, flow birefringence and dielectric loss,” *J. Chem. Phys.* **24**, 269 (1956).
- ¹⁹⁷K. Kroy and E. Frey, “Dynamic scattering from solutions of semiflexible polymers,” *Phys. Rev. E* **55**, 3092 (1997).
- ¹⁹⁸R. G. Winkler, “Analytical calculation of the relaxation dynamics of partially stretched flexible chain molecules: Necessity of a wormlike chain description,” *Phys. Rev. Lett.* **82**, 1843 (1999).
- ¹⁹⁹S. K. Anand and S. P. Singh, “Conformation and dynamics of a self-avoiding active flexible polymer,” *Phys. Rev. E* **101**, 030501 (2020).
- ²⁰⁰E. P. Petrov, T. Ohrt, R. G. Winkler, and P. Schwille, “Diffusion and segmental dynamics of double-stranded DNA,” *Phys. Rev. Lett.* **97**, 258101 (2006).
- ²⁰¹D. G. Grier, “A revolution in optical manipulation,” *Nature* **424**, 810 (2003).
- ²⁰²S. Ganguly, L. S. Williams, I. M. Palacios, and R. E. Goldstein, “Cytoplasmic streaming in *Drosophila* oocytes varies with kinesin activity and correlates with the microtubule cytoskeleton architecture,” *Proc. Natl. Acad. Sci. USA* **109**, 15109 (2012).
- ²⁰³H. Ennomani, G. Letort, C. Guérin, J.-L. Martiel, W. Cao, F. Nédélec, E. M. De La Cruz, M. Théry, and L. Blanchoin, “Architecture and connectivity govern actin network contractility,” *Curr. Biol.* **26**, 616 (2016).
- ²⁰⁴K.-T. Wu, J. B. Hishamunda, D. T. N. Chen, S. J. DeCamp, Y.-W. Chang, A. Fernández-Nieves, S. Fraden, and Z. Dogic, “Transition from turbulent to coherent flows in confined three-dimensional active fluids,” *Science* **355**, eaal1979 (2017).
- ²⁰⁵J. M. Belmonte, M. Leptin, and F. Nédélec, “A theory that predicts behaviors of disordered cytoskeletal networks,” *Mol. Syst. Biol.* **13**, 941 (2017).
- ²⁰⁶L. Huber, R. Suzuki, T. Krüger, E. Frey, and A. R. Bausch, “Emergence of coexisting ordered states in active matter systems,” *Science* **361**, 255 (2018).
- ²⁰⁷P. Guillamat, Ž. Kos, J. Hardoüin, J. Ignés-Mullol, M. Ravník, and F. Sagués, “Active nematic emulsions,” *Sci. Adv.* **4**, eaao1470 (2018).
- ²⁰⁸F. Peruani, A. Deutsch, and M. Bär, “Nonequilibrium clustering of self-propelled rods,” *Phys. Rev. E* **74**, 030904 (2006).
- ²⁰⁹F. Ginelli, F. Peruani, M. Bär, and H. Chaté, “Large-scale collective properties of self-propelled rods,” *Phys. Rev. Lett.* **104**, 184502 (2010).
- ²¹⁰H. H. Wensink, J. Dunkel, S. Heidenreich, K. Drescher, R. E. Goldstein, H. Löwen, and J. M. Yeomans, “Meso-scale turbulence in living fluids,” *Proc. Natl. Acad. Sci. USA* **109**, 14308 (2012).
- ²¹¹H. H. Wensink and H. Löwen, “Emergent states in dense systems of active rods: from swarming to turbulence,” *J. Phys.: Condens. Matter* **24**, 460130 (2012).
- ²¹²M. Abkenar, K. Marx, T. Auth, and G. Gompper, “Collective behavior of penetrable self-propelled rods in two dimensions,” *Phys. Rev. E* **88**, 062314 (2013).
- ²¹³C. Abaurrea Velasco, M. Abkenar, G. Gompper, and T. Auth, “Collective behavior of self-propelled rods with quorum sensing,” *Phys. Rev. E* **98**, 022605 (2018).
- ²¹⁴M. Bär, R. Großmann, S. Heidenreich, and F. Peruani, “Self-propelled rods: Insights and perspectives for active matter,” *Annu. Rev. Condens. Matter Phys.* **11**, 441 (2020).
- ²¹⁵T. B. Liverpool, A. C. Maggs, and A. Ajdari, “Viscoelasticity of solutions of motile polymers,” *Phys. Rev. Lett.* **86**, 4171 (2001).
- ²¹⁶H. Jiang and Z. Hou, “Motion transition of active filaments: rotation without hydrodynamic interactions,” *Soft Matter* **10**, 1012 (2014).
- ²¹⁷R. Chelakkot, A. Gopinath, L. Mahadevan, and M. F. Hagan, “Flagellar dynamics of a connected chain of active, polar, Brownian particles,” *J. R. Soc. Interf.* **11**, 20130884 (2014).
- ²¹⁸R. E. Isele-Holder, J. Elgeti, and G. Gompper, “Self-propelled worm-like filaments: spontaneous spiral formation, structure, and dynamics,” *Soft Matter* **11**, 7181 (2015).
- ²¹⁹O. Duman, R. E. Isele-Holder, J. Elgeti, and G. Gompper, “Collective dynamics of self-propelled semiflexible filaments,” *Soft Matter* **14**, 4483 (2018).
- ²²⁰K. R. Prathyusha, S. Henkes, and R. Sknepnek, “Dynamically generated patterns in dense suspensions of active filaments,” *Phys. Rev. E* **97**, 022606 (2018).
- ²²¹S. K. Anand and S. P. Singh, “Structure and dynamics of a self-propelled semiflexible filament,” *Phys. Rev. E* **98**, 042501 (2018).
- ²²²M. S. E. Peterson, M. F. Hagan, and A. Baskaran, “Statistical properties of a tangentially driven active filament,” *J. Stat. Mech. Theor. Exp.* **2020**, 013216 (2020).
- ²²³H. Risken, *The Fokker-Planck Equation* (Springer, Berlin, 1989).
- ²²⁴C. Philipps, G. Gompper, and R. G. Winkler, “Analytical studies of polar active filaments,” in progress (2020).
- ²²⁵R. E. Isele-Holder, J. Jäger, G. Saggiorato, J. Elgeti, and G. Gompper, “Dynamics of self-propelled filaments pushing a load,” *Soft Matter* **12**, 8495 (2016).
- ²²⁶S. K. Anand and S. P. Singh, “Behavior of active filaments near solid-boundary under linear shear flow,” *Soft Matter* **15**, 4008 (2019).
- ²²⁷H. Jiang and Z. Hou, “Hydrodynamic interaction induced spontaneous rotation of coupled active filaments,” *Soft Matter* **10**, 9248 (2014).
- ²²⁸J. Clopes Llahi, G. Gompper, and R. G. Winkler, “Swimming behavior of squirmer dumbbells,” in preparation (2020).
- ²²⁹T. Ishikawa, “Stability of a dumbbell micro-swimmer,” *Micro-machines* **10**, 33 (2019).
- ²³⁰R. Matas Navarro and I. Pagonabarraga, “Hydrodynamic interaction between two trapped swimming model micro-organisms,” *Eur. Phys. J. E* **33**, 27 (2010).
- ²³¹J. G. Kirkwood and J. Riseman, “The intrinsic viscosities and diffusion constants of flexible macromolecules in solution,” *J. Chem. Phys.* **16**, 565 (1948).
- ²³²D. Saintillan, M. J. Shelley, and A. Zidovska, “Extensile motor activity drives coherent motions in a model of interphase chromatin,” *Proc. Natl. Acad. Sci. USA* **115**, 11442 (2018).
- ²³³A. Wysocki, R. G. Winkler, and G. Gompper, “Cooperative motion of active Brownian spheres in three-dimensional dense suspensions,” *EPL* **105**, 48004 (2014).
- ²³⁴J. Stenhammar, D. Marenduzzo, R. J. Allen, and M. E. Cates, “Phase behaviour of active Brownian particles: the role of dimensionality,” *Soft Matter* **10**, 1489 (2014).
- ²³⁵A. Wysocki, R. G. Winkler, and G. Gompper, “Propagating interfaces in mixtures of active and passive Brownian particles,” *New J. Phys.* **18**, 123030 (2016).
- ²³⁶M. E. Cates and J. Tailleur, “Motility-induced phase separation,” *Annu. Rev. Condens. Matter Phys.* **6**, 219 (2015).
- ²³⁷P. Digregorio, D. Levis, A. Suma, L. F. Cugliandolo, G. Gonnella, and I. Pagonabarraga, “Full phase diagram of active Brownian disks: From melting to motility-induced phase separation,” *Phys. Rev. Lett.* **121**, 098003 (2018).
- ²³⁸D. Saintillan and M. J. Shelley, “Instabilities and pattern formation in active particle suspensions: Kinetic theory and continuum simulations,” *Phys. Rev. Lett.* **100**, 178103 (2008).
- ²³⁹G. Vliegert, A. Ravichandran, M. Ripoll, T. Auth, and G. Gompper, “Filamentous active matter: Band formation, bending, buckling, and defects,” *Sci. Adv.*, in press (2020), [arXiv:1902.07904 \[cond-mat.soft\]](https://arxiv.org/abs/1902.07904).
- ²⁴⁰M. F. Copeland and D. B. Weibel, “Bacterial swarming: a model system for studying dynamic self-assembly,” *Soft Matter* **5**, 1174 (2009).
- ²⁴¹D. B. Kearns, “A field guide to bacterial swarming motility,” *Nat. Rev. Microbiol.* **8**, 634 (2010).
- ²⁴²M. E. Cates and F. C. MacKintosh, “Active soft matter,” *Soft Matter* **7**, 3050 (2011).
- ²⁴³G. Duclos, R. Adkins, D. Banerjee, M. S. E. Peterson, M. Varghese, I. Kolvin, A. Baskaran, R. A. Pelcovits, T. R. Powers,

- A. Baskaran, F. Toschi, M. F. Hagan, S. J. Streichan, V. Vitelli, D. A. Beller, and Z. Dogic, "Topological structure and dynamics of three-dimensional active nematics," *Science* **367**, 1120 (2020).
- ²⁴⁴S. Das and A. Cacciuto, "Deviations from blob scaling theory for active Brownian filaments confined within cavities," *Phys. Rev. Lett.* **123**, 087802 (2019).
- ²⁴⁵J. Stenhammar, R. Wittkowski, D. Marenduzzo, and M. E. Cates, "Activity-induced phase separation and self-assembly in mixtures of active and passive particles," *Phys. Rev. Lett.* **114**, 018301 (2015).
- ²⁴⁶D. Rogel Rodriguez, F. Alarcón, R. Martínez, J. Ramírez, and C. Valeriani, "Phase behaviour and dynamical features of a two-dimensional binary mixture of active/passive spherical particles," *Soft Matter* **16**, 1162 (2020).
- ²⁴⁷N. Nikola, A. P. Solon, Y. Kafri, M. Kardar, J. Tailleur, and R. Voituriez, "Active particles with soft and curved walls: Equation of state, ratchets, and instabilities," *Phys. Rev. Lett.* **117**, 098001 (2016).
- ²⁴⁸Y.-q. Xia, Z.-l. Shen, W.-d. Tian, and K. Chen, "Unfolding of a diblock chain and its anomalous diffusion induced by active particles," *J. Chem. Phys.* **150**, 154903 (2019).
- ²⁴⁹Y.-Q. Xia, W.-D. Tian, K. Chen, and Y.-Q. Ma, "Globule-stretch transition of a self-attracting chain in the repulsive active particle bath," *Phys. Chem. Chem. Phys.* **21**, 4487 (2019).
- ²⁵⁰Y. Fily, A. Baskaran, and M. F. Hagan, "Dynamics of self-propelled particles under strong confinement," *Soft Matter* **10**, 5609 (2014).
- ²⁵¹A. Y. Grosberg and J. F. Joanny, "Nonequilibrium statistical mechanics of mixtures of particles in contact with different thermostats," *Phys. Rev. E* **92**, 032118 (2015).
- ²⁵²C. P. Brangwynne, T. J. Mitchison, and A. A. Hyman, "Active liquid-like behavior of nucleoli determines their size and shape in *xenopus laevis* oocytes," *Proc. Natl. Acad. Sci. USA* **108**, 4334 (2011).
- ²⁵³H. Falahati and E. Wieschaus, "Independent active and thermodynamic processes govern the nucleolus assembly in vivo," *Proc. Natl. Acad. Sci. USA* **114**, 1335 (2017).
- ²⁵⁴W. M. Babinchak and W. K. Surewicz, "Liquid-liquid phase separation and its mechanistic role in pathological protein aggregation," *J. Mol. Biol.* (2020), 10.1016/j.jmb.2020.03.004.
- ²⁵⁵F. S. Bates and G. H. Fredrickson, "Block copolymer thermodynamics: Theory and experiment," *Annu. Rev. Phys. Chem.* **41**, 525 (1990).
- ²⁵⁶Y. Mai and A. Eisenberg, "Self-assembly of block copolymers," *Chem. Soc. Rev.* **41**, 5969 (2012).
- ²⁵⁷A. Cavagna and I. Giardina, "Bird flocks as condensed matter," *Annu. Rev. Condens. Matter Phys.* **5**, 183 (2014).
- ²⁵⁸G. Popkin, "The physics of life," *Nature* **529**, 16 (2016).
- ²⁵⁹A. N. Kolmogorov, V. Levin, J. C. R. Hunt, O. M. Phillips, and D. Williams, "The local structure of turbulence in incompressible viscous fluid for very large Reynolds numbers," *Proc. R. Soc. A* **434**, 9 (1991).
- ²⁶⁰H. M. López, J. Gachelin, C. Douarche, H. Auradou, and E. Clément, "Turning bacteria suspensions into superfluids," *Phys. Rev. Lett* **115**, 028301 (2015).
- ²⁶¹V. A. Martínez, E. Clément, J. Arlt, C. Douarche, A. Dawson, J. Schwarz-Linek, A. K. Creppy, V. Škultéty, A. N. Morozov, H. Auradou, and W. C. K. Poon, "A combined rheometry and imaging study of viscosity reduction in bacterial suspensions," *Proc. Natl. Acad. Sci. USA* **117**, 2326 (2020).
- ²⁶²A. Martín-Gómez, G. Gompper, and R. G. Winkler, "Active Brownian filamentous polymers under shear flow," *Polymers* **10**, 837 (2018).
- ²⁶³A. Deblais, S. Woutersen, and D. Bonn, "Rheology of entangled active polymer-like t. tubifex worms," *Phys. Rev. Lett.* **124**, 188002 (2020).